REGULATORY ROLE OF PARP-1 IN ISLET DIFFERENTIATION FROM PANCREATIC PROGENITORS

CHAPTER 4

Chapter 4

Regulatory role of PARP-1 in Islet Differentiation from pancreatic progenitors

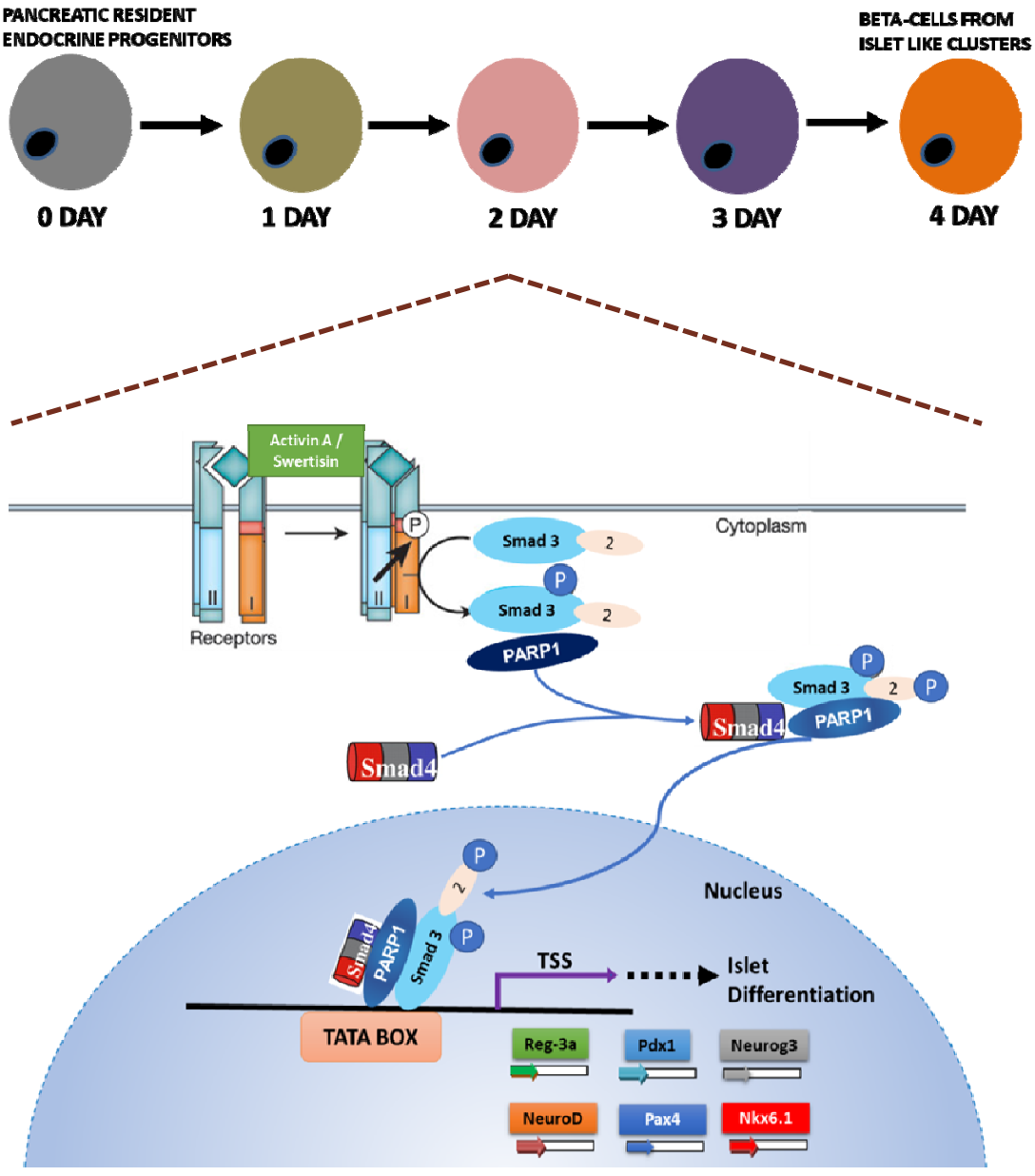

4.1. Introduction

Islet replacement therapy demands the need to optimize ways to generate islet mass from various stem/progenitor sources for replenishment of lost beta cells (Shapiro et al., 2017; Soria et al., 2001). As mentioned previously and supported by our previous lab reports a sequential and timely expression of key transcription factors is essential to direct stem/progenitors towards an insulin producing beta cell fate. It is well documented that all the transcription factors essential in pancreatic development and in maintenance of beta cell function and homeostasis act synergistically (Cerf, 2006) (Fig 4.1). Further, these transcription factors are regulated by certain other factors and PARP-1 could be one them. Okamoto in 1989 first reported PARP-1's role in islet regeneration in an in vivo model where it was observed to regulate the Reg gene transcription and thereby modulate the regeneration in islet of Langerhans (Takasawa and Okamoto, 2002).

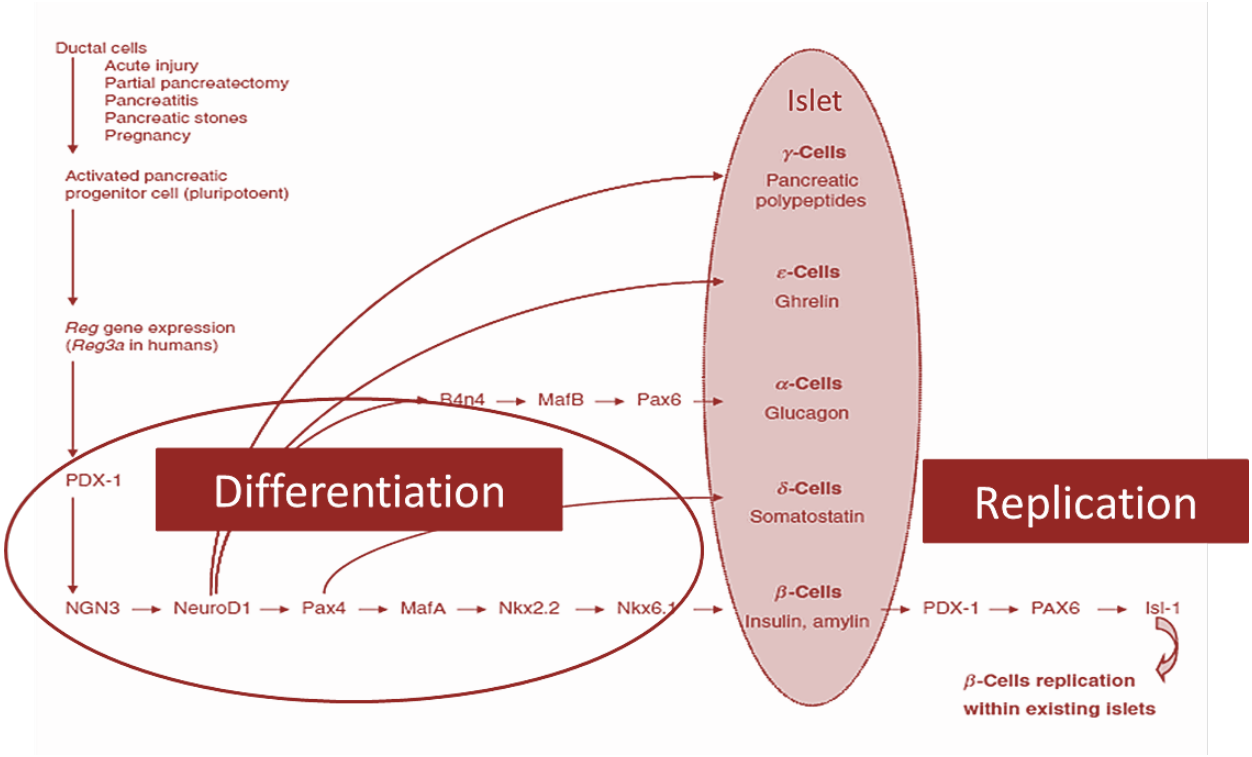

Figure 4.1: Transcription Factors in Islet differentiation: Schematic representation of essential transcription factors governing beta cell fate during islet differentiation. Adapted from (Levetan, 2010) Levetan C., 2010.

PARP-1, a ubiquitous nuclear protein is popularly identified for its role in DNA repair and cell death but slowly this stereotype for this protein has seen a shift towards its lesser known functions which involve chromatin modulation, control of transcription factors and epigenetic control (Fig 4.2). Several earlier studies have implicated PARP-1 in different stages of diabetes from development of the disease to its complications (Kraus and Lis, 2003; Krishnakumar and Kraus, 2010). It was observed that PARP-1 knockout mice were resistant to STZ induced insulin dependent diabetes mellitus (Shall and de Murcia, 2000). Further, islets from PARP-1 null mice were found to be more resistant to the toxicity of nitric oxide and reactive oxygen intermediates (Uchigata et al., 1982; Yamamoto and Okamoto, 1980).

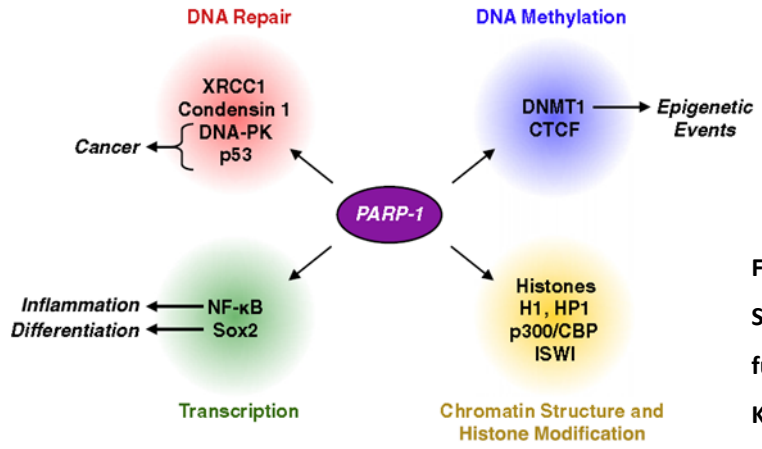

Figure 4.2: Varied functions of PARP-1: Schematic representation of various functions of PARP-1 protein. Krishnakumar and Kraus, 2010.

The first study was in 1984 where in 90% pancreatectomised rat model PARP inhibitors ameliorated the diabetic condition and later Reg gene was identified as an essential factor for regeneration of pancreatic tissue (Watanabe et al., 1994; Yonemura et al., 1984). It was demonstrated that PARP-1, interacts with the nuclear proteins forming the transcription complex on Reg gene. It negatively regulated Reg's expression by auto-PARylating itself. However, incorporating PARP inhibitors prevented auto-PARylation, thus stabilizing the transcription complex for Reg gene expression (Akiyama et al., 2001). This interaction of PARP-1 with Reg gene is the Okamoto model for beta cell regeneration (Takasawa and Okamoto, 2002). Although, this study was performed in the *in vivo* condition, its

implications for PARP-1 being a regulatory partner in the transcription complex during pancreatic regeneration was vital, which could be extrapolated in the *in vitro* islet differentiation studies from various stem/progenitors to identify other such regulatory functions of PARP-1.

Further, it was observed that supplementing INS-1 in beta cells with PARP inhibitors increases insulin promoter activity. It was later confirmed that PARP inhibitors increased the binding of MafA to the promoter of INS-1 gene which enhanced its transcription (Ye et al., 2006). Also, in context of diabetic complications, PARP inhibitors have shown efficacy in endothelial dysfunction, retinopathy, nephropathy, neuropathy and cardiomyopathy (Garcia Soriano et al., 2001; Kiss and Szabo, 2005; Li et al., 2005; Minchenko et al., 2003; Obrosova et al., 2004; Xiao et al., 2004). It has been observed that PARP-1 PARylates GAPDH and inhibit its action, which is alleviated in the presence of PARP inhibitors thereby suppressing glucotoxicity by inhibiting major pathways of hyperglycemic damage (Du et al., 2003). Further, Protective effect of PARP inhibition on vascular and retinal endothelial, kidney tubules, neuroendothelial, Schwaan cells and myocardium seems to be have the common mechanisms; conservation of NAD+, the cellular energy pool, prevention or inhibition of pro-inflammatory pathways viz. cytokines, adhesion molecules, mononuclear cell infiltration etc., which are suppressed by PARP inhibition by suppressing NF-KB activation (Kiss and Szabo, 2005).

Classically, TGF-β is known to play important role in proliferation, differentiation and migration in embryonic development and adult tissue homeostasis (Watabe and Miyazono, 2009) and , TGF-β signalling also plays pivotal role during islet differentiation and neogenesis from stem cells (Brown and Schneyer, 2010; Kim and Hebrok, 2001b) . As discussed above PARP-1 plays a crucial role in regulating islet neogenesis (Takasawa and

Okamoto, 2002) and also demonstrated to interact with SMAD3 and SMAD4, as a negative and positive regulator (Huang et al., 2011; Lönn et al., 2010; Zhang et al., 2013).

However, none have addressed the possible role of PARP-1 in islet neogenesis from stem/progenitor cells. Based on the results generated so far, in the lab, it is evident that PARP-1 is an essential factor for islet differentiation from PANC-1 cell line (Nidheesh Dadheech Thesis, 2013). Hence, to have a better understanding of mechanisms that influence islet neogenesis from primary cultured progenitor cells obtained from mice pancreas, we further explored the mechanism of PARP-1 interaction with specific and crucial genes governing beta cell fate from progenitor cells by silencing PARP-1 and generating PARP-1 KD stem progenitors and using PARP-1 inhibitors against its enzyme activity to elucidate its mechanism in islet differentiation from stem/progenitors (PREPs) (Fig 4.3).

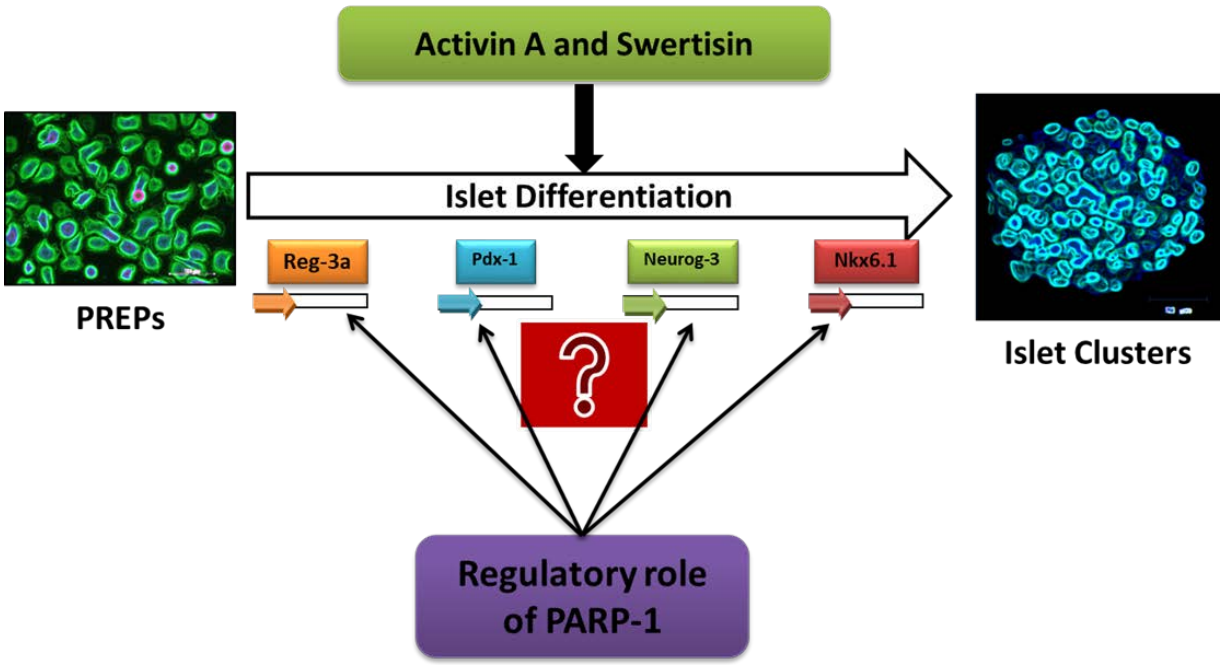

Figure 4.3: Experimental Hypothesis: PARP-1 expression is essential in islet differentiation and could be playing a regulatory role with respect to the expression of key transcription factors during islet differentiation from stem/progenitors.

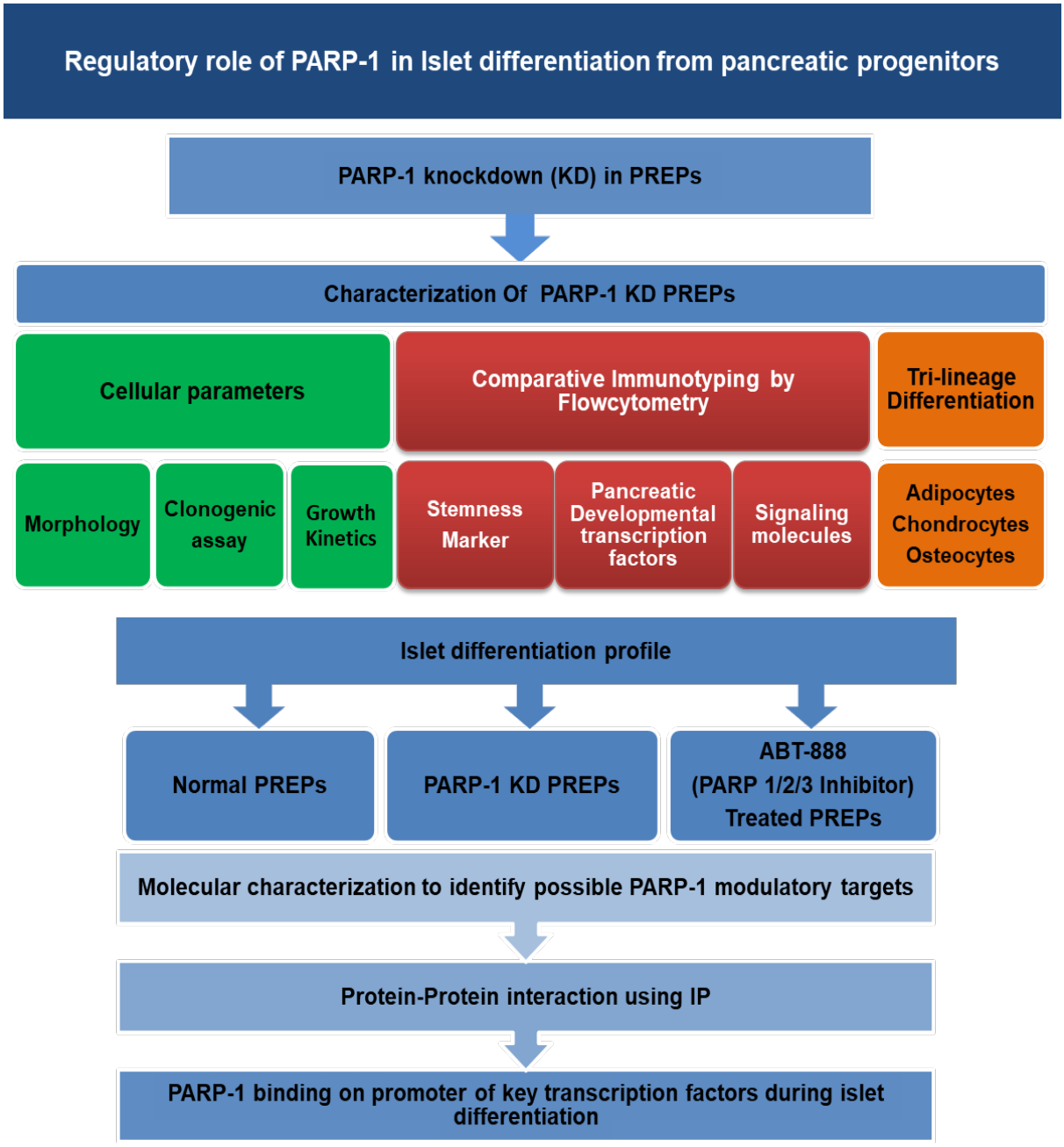

Figure 4.4: Experimental Design for Chapter 4.

4.2. Material and methods

4.2.1. Experimental Design:

PARP-1 gene was silenced in PREPs using shRNA vector. Comparative characterization of normal PREPs and PARP-1 KD PREPs was performed for their morphology, proliferative potential, various markers and differentiation potential. Comparative assessment of islet differentiation potential between normal PREPs, PRAP-1 KD PREPs and ABT-888 treated

PREPs to understand the role of PARP-1 was done. Molecular characterization to identify possible regulatory targets was performed during islet differentiation, which was confirmed in PANC-1 cells. Co-Immunoprecipitation to explore and identify possible PARP-1 interacting partners was performed followed by Chromatin Immunoprecipitation to confirm PARP-1's regulatory role in transcription control during islet differentiation (Fig 4.4).

4.2.2. RNAi vectors and Plasmids:

To understand the mechanism of PARP-1 in islet differentiation, PARP-1 gene was knockdown using specific shRNA against PARP-1 gene. DNA vector-based RNAi approach, established and gifted by Dr. Girish M Shah lab, Universite Laval, Quebec, Canada, to stably and very significantly knock down PARP-1 in PREPs (pSIP912 PARP-1 KD PREP clone) and control PARP-1-replete (pBSU6 clone) having only vector construct without shRNA (Shah et al., 2005). Further, we also received the PARP-1 recovery vector from Dr. Shah, which was immune to the action of siRNA within pSIP912 due to a point mutation at its target site. The vector maps and sequence of shRNA chosen against PARP-1 gene is given in Appendix 1.

4.2.3. Cell culture maintenance:

PREPs were maintained in high glucose DMEM supplemented with 10% Fetal Bovine Serum. PANC-1 cells were cultured and maintained as described in chapter 3. PANC-1 cells have similar growth condition as PREPs and were maintained similarly.

4.2.4. Transfection to generate PARP-1 stable knockdown clones, siRNA generated transient clone in PREPs and recovery using recovery vector:

We transfected PREPs with GFP harboring plasmid pEGFP-N1 (Clontech), so that the cells could be differentiated from those of the host. Five hundred thousand cells were co-transfected with 0.2 µg pEGFP-N1 and 1 µg pSIP912/pBSU6 plasmid DNA in a ratio of 1:5 using Neon electroporation system (Invitrogen) with one pulse at a pulse voltage of 1400 V

with pulse width 20 ms and plating the cells on a 3.5 cm^2 dish, according to the manufacturer's protocol. Following the transfection, stably GFP expressing clones were selected by growing them in media containing G418 at 300 µg/mL concentration. They were then seeded at a very low density with high selection of 600 µg/mL G418 till separate colonies were seen on the plate. The GFP+ve colony clones were purified using clonal discs and scaled up and screened for PARP-1 knockdown by western blotting. For recovery PARP-1 KD clone 4 was transfected using above conditions with the recovery vector pRSIP and screened for recovered expression of PARP-1 by western blotting. Similarly siRNA based silencing of PARP-1 using Neon was performed in PREPs.

4.2.5. Clonogenic Assay:

7500 cells were seeded in a 10 cm^2 culture dish in proliferative medium for a period of three weeks. The colonies formed were washed with PBS and stained with 0.5% solution of crystal violet. Colony count was taken and data was analysed.

4.2.6. Cell count and growth kinetics:

Approximately 80% confluent PREPs both normal and PARP-1 KD were trypsinized with 0.1% Trypsin EDTA solution and counted under an inverted phase contrast microscope (Nikon TE2000, Japan) on neubauer chamber using 0.05% trypan blue dye. Thirty thousand cells were seeded into each well of 24-well plates for growth curve studies. Cells were eventually trypsinized and counted at different time points (0h, 24h, 48h, 72h, 96h, 120h and 144h). Cell counts were then plotted versus time to establish the growth curve of cells. Growth curve of normal PREPs was compared with that of PARP-1 KD PREPs. Doubling time of both the cells were also determined in the exponential growth phase using the algorithm ln (Nt-N0) ln (t), where Nt and N0 were number of cells at final time point and at

initial seeding point respectively, and t was time period in hours for which cell counts were recorded.

4.2.7. Immunophenotyping:

A comparative immunophenotyping of stemness markers, pancreatic developmental markers and signaling makers was performed between normal PREPs and PARP-1 KD PREPs by flowcytometry as described in chapter 3, section 3.2.6.

4.2.8. Trilineage Differentiation:

A comparative trilineage differentiation was performed between normal PREPs and PARP-1 KD PREPs as described previously in chapter 3, section 3.2.7.

4.2.9. Islet Differentiation

Islet differentiation protocol was followed as described in chapter 3, section 3.2.8 with DMEM KO in 1%BSA, ITS and Activin A/Swertisin containing media.

4.2.10. Protein extraction and Western blotting

A comparative temporal protein profiling was performed to identify possible PARP-1 regulatory targets between normal PREPs and PARP-1 KD PREPs during islet differentiation. Similar study was done with PANC-1 cells to confirm PREP data. Western blotting was performed as previously described in chapter 3, section 3.2.9.

4.2.11. Immunocytochemistry staining:

Functional characterization of mature islets was performed, chapter 3, section 3.2.5.

4.2.12. Gene expression study:

Undifferentiated PANC-1 cells and differentiated islet like clusters at day 5 were subjected to RNA isolation using TriSoln (Sigma Alrich, USA) followed by its quantification. 2 µg of total RNA was reverse transcribed into cDNA using first strand c-DNA synthesis kit

(Fermentas INC., USA) as per manufacturer's instruction for gene expression profiling was semi quantitative RT-PCR for a Taqman gene array for transcriptome analysis during islet differentiation. The details of the gene array are described in Appendix 2.

4.2.15. C-peptide release assay:

As described in chapter 3, section 3.2.11

4.2.14. Selecting ABT-888 dose and MTT assay:

ABT-888 was preincubated at doses from 5 nM to 5 μM with PREPs 15 min before treatment with 100 μM H_2O_2. Cells were harvested on ice after 30 min of incubation at 37˚C CO_2 incubator with 5% CO_2. The doses were screened for effective abatement of PARylation. Also, same doses were screened for toxicity in PREPs on incubation for 24 hr. with MTT assay. Extent of cell death and effect of PARP-1/2/3 inhibitor ABT-888 were determined by MTT assay (Roche). PREPs were seeded into 96-well plates at a density of ten thousand cells per well in complete medium. MTT reagent was added in culture in each well after 24 hours incubation with different concentrations of ABT-888. The optical density values were analyzed 4 hr. after the MTT reaction using Multiskan PC (Thermo Lab), and percentage viability histogram was plotted.

4.2.15. Effect of SIS3 on PREPs during islet differentiation:

SIS3 is a potent drug that inhibits phosphorylation of Smad3. In order to understand the significance of Smad3 phosphorylation SIS3 was added to the differentiation media of PREPs during islet differentiation in both Activin A and Swertisin groups. The dose of SIS3 was taken from a previous report (Jinnin et al., 2006), which was screened for possible toxicity by MTT assay as described above. 10 μM SIS3 was used to inhibit phosphorylation in islet differentiation from PREPs.

4.2.16. Fractionation of Extra nuclear and Nuclear fraction during islet differentiation:

Differentiated islet like clusters were harvested in buffer A (10 mM Hepes of pH 7.8, 10 mM KCl, 1.5 mM $MgCl_2$, 0.34 M sucrose, 10% glycerol, 0.1% triton x 100, 1 mM PMSF, 1X protease inhibitor, 10 mM β-glycerophosphate, 10 mM Sodium Fluoride, 1 mM Sodium Orthovanadate) at 4˚C and incubated for 7 min to acquire whole cell extract. 50 µl of aliquot from this extract was preserved at -20 ˚C. The rest sample was centrifuged at 1000g for 5 min at 4˚C where cytoplasmic extract in supernatant and pellet containing nucleus was obtained. The pellet was again washed with buffer A and then resuspended in 400ul Buffer B (50 mM Tris-HCl pH 7.8, 1 mM EDTA, 450 mM NaCl, 0.34 M sucrose, 10% glycerol, 0.5% Nonidet, 1 mM PMSF, 1X protease inhibitor, 10 mM β-glycerophosphate, 10 mM Sodium Fluoride, 1 mM Sodium Orthovanadate) followed by incubation for 30 min at 4˚C to obtain nuclear extract. All the extracts were sonicated and stored at -20˚C till further use.

4.2.17. Co-Immunoprecipitation with PARP-1 antibody during islet differentiation:

Dynabeads procured from Invitrogen were resuspended, 1 mg per sample beads were magnetized and washed with PBST (PBS + 0.1% Tween 20) before adding 1 µg antibody in final volume of 200 µl. Beads were incubated with antibody (IgG as negative control) at RT for 10 min on rotary tube rollers. Further, these beads were magnetized and the supernatant was discarded followed by washing with 1ml of PBS-T for 3 times. The antigen-containing lysate (100 µg/200 µl) was added to this antibody coated beads and rotated overnight at 4˚C. After incubation, washing was performed with 1ml of PBS-T and supernatant was discarded. Before the last magnetization, resuspended beads were transferred to a new tube and spin down for several seconds and the beads were magnetized for the removal of residual buffer from the tubes. Proteins were eluted from these beads using 40 µl 1x Laemmli buffer and incubation for 10 min at 70°C followed by magnetization of beads and collection of eluent. Proceed for western blotting.

4.2.18. Chromatin Immunoprecipitation during Islet differentiation from PREPs:

For PARP-1 ChIP, both undifferentiated PREPs (4 x 10^6 cells) and differentiated Islet clustered from (4 x 10^6 cells) at 3rd day of differentiation from both Activin A and Swertisin groups were fixed with 1% formaldehyde for 10 min at RT, quenched with 125 mM Glycine for 5 min at RT. The rest of the sample processing was performed by using Pierce Magnetic ChIP kit (Thermo Scientific) as per manufacturer's instruction. Summarizing the protocol, after crosslinking the cells and harvesting, cells membrane was lysed and the nuclei was subjected to MNase treatment (8 units/4 x 10^6 cells) followed by sonication to break open the nuclei, sonication was performed using a cup horn sonicator probe on maximum amplitude for 30 min with 30 sec on off cycles on ice water constantly. 100 µg DNA was incubated with 2 µg PARP-1 antibody for overnight incubation at 4˚C with rotation. Protein A/G magnetic beads were added to the DNA fragment-Antibody solution, incubated at 4˚C for 2 hr. Beads were collected, washed and the DNA bound to PARP-1 protein pooled using Antibody was eluted. Crosslinking was reversed by treating with Proteinase K. DNA clean-up was performed using columns and samples were analysed using real time PCR. The data was represented as %input. Values were averaged from three independent experiments. See Table 4.1 for ChIP primers and Appendix 3.

4.3. Results

4.3.1. Silencing of PARP-1 gene in PREPs using RNA Interference technology:

In order to understand the role of PARP-1 in Islet differentiation we performed silencing of PARP-1gene in PREPs (passage #10) by co-transfecting pSIP912 vector and pBSU6 empty vector with pEGFP-N1 respectively. Electroporation was performed by using Neon transfection system (Invitrogen, Thermo Fisher Scientific) which yielded 56% transfection efficiency analyzed with Tali, cell counter (Invitrogen, Thermo Fisher Scientific). The transfected cells were seeded in a very low density under a high G418 selection of 800 µg/ml.

The cells yielded in separate colonies which were screened for GFP+ve signal and picked up for expanding individually under G418 selection pressure at 300 µg/ml. These individual clones were then screened for silencing of PARP-1 gene by performing western blotting (Fig 4.5). The clones in which PARP-1 was silenced were selected and cultured further. Clones 4 and 33 were almost complete knockdown clones of PARP-1 and clones 11,12,24,35 and 36 were partial knockdowns. We observed that clone 4 had the maximum silencing of PARP-1, which was then used to perform rest of the experiments. In order to confirm a stable knockdown of PARP-1 in these cells we again screened clone 4 with western blot for expression of PARP-1 after 4 passages which showed no PARP-1 expression. This confirmed a stable knockdown (KD) of PARP-1 in PREPs (Fig 4.6).

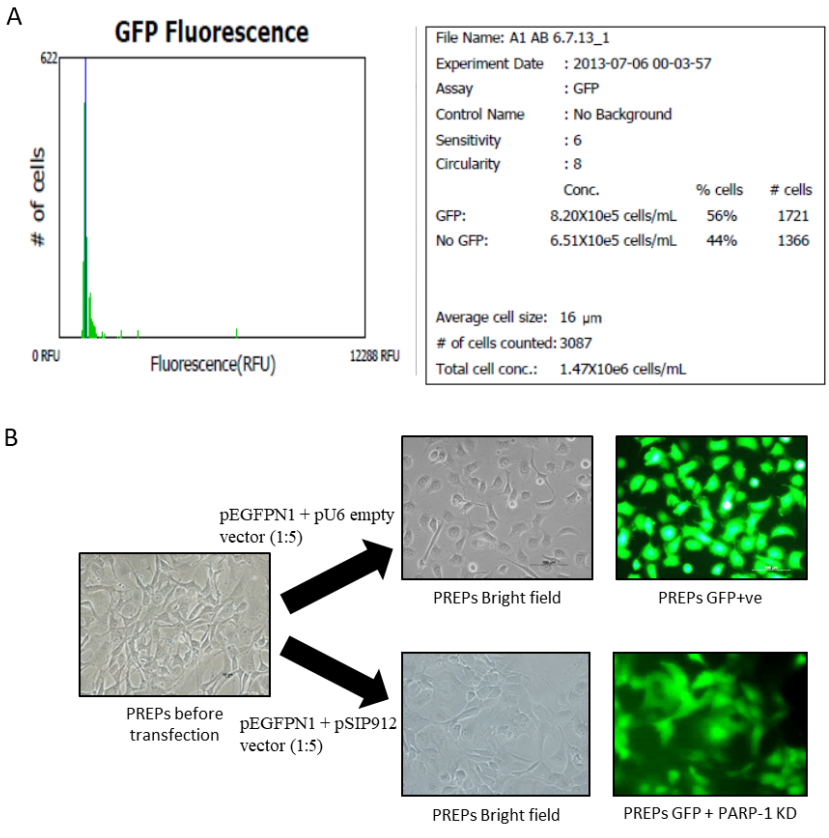

Figure 4.5: Co-transfection Efficiency and clone purification of PREPs: (A) Percentage of transfection efficiency analysed by Tali, image based cell counter. (B) The figure demonstrated purified GFP positive vector control PREPs and GFP positive PARP1 knockdown PREPs respectively.

4.3.2. Characterization of PREP clone 4 (PARP-1 KD):

After achieving stable knockdown of PARP-1 gene in PREPs, we were interested in observing any changes with respect to the cell morphology, proliferative potential and differentiation potential when compare to the normal PARP-1 positive normal PREPs.

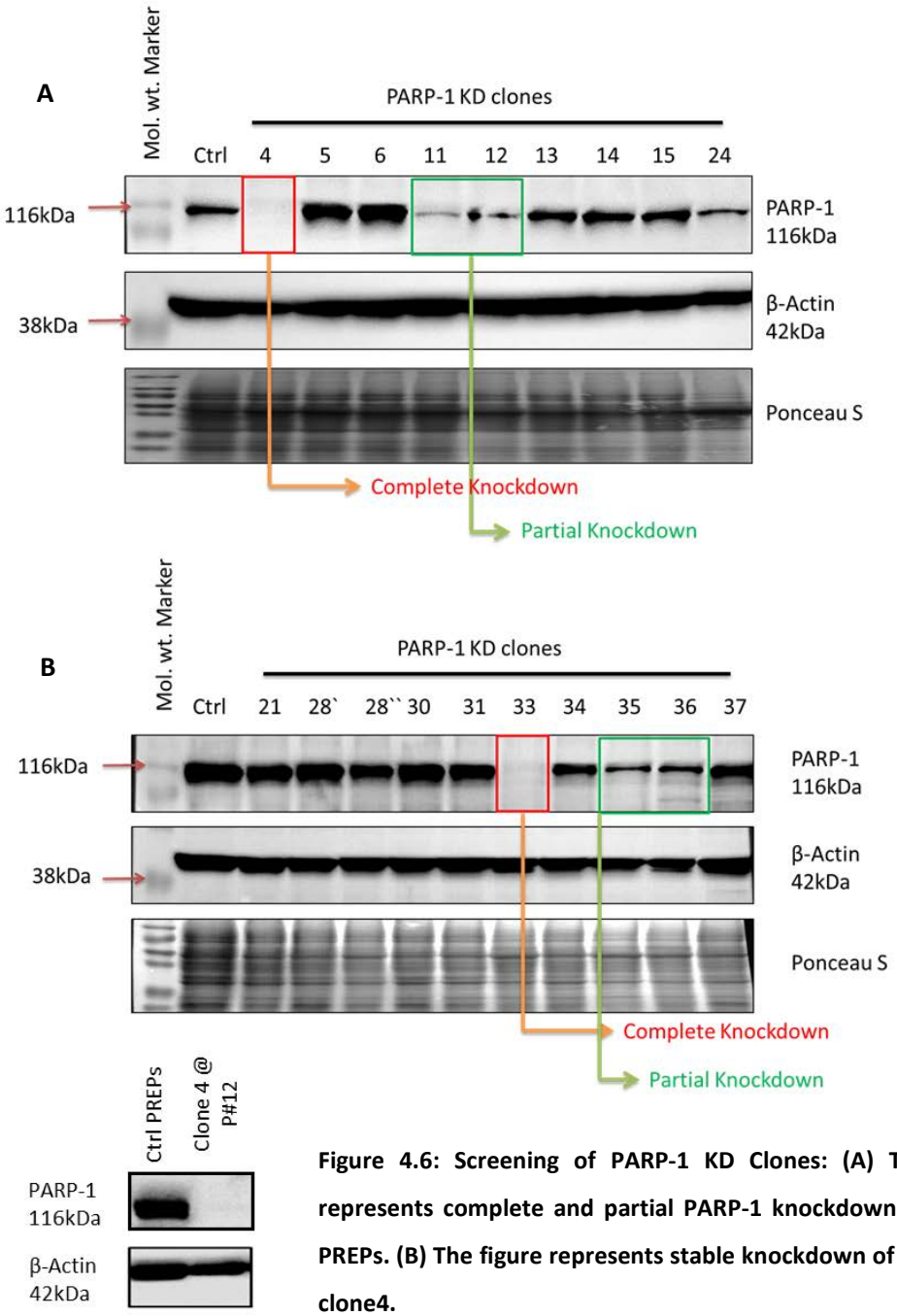

Figure 4.6: Screening of PARP-1 KD Clones: (A) The figure represents complete and partial PARP-1 knockdown clones of PREPs. (B) The figure represents stable knockdown of PARP-1 in clone4.

4.3.2.1. Comparative study of PARP-1 normal & KD PREPs to assess morphological changes and alteration to their proliferative potential:

We observed a marked change in the basic morphology of the PARP-1 KD cells when compared to their parent phenotype. Clonogenic assay was performed to assess the survivability and proliferative potential of PREPs after the knockdown. Both PARP-1 normal and KD cells (7.5×10^3) were seeded on $10cm^2$ dishes respectively and incubated for a period of 2 weeks. We observed a significant reduction in number and size and number of the colonies that were formed indicating loss in proliferative potential in the PARP-1 KD cells.

Further, growth kinetics for both the cell types was performed simultaneously for a period over 144 h with cell counts every 24 h. We observed that the PARP-1KD cells were significantly slower to proliferate. Also, the doubling time of the PARP-1KD cells was found to have significantly increased to 34.4 hr against PARP-1 normal cells 21.94 hr (Fig 4.7).

4.3.2.2. Comparative study of PARP-1 normal & KD to assess deviations in their stemness and pancreatic endocrine markers:

Once it was clear that the cellular phenotype after the knockdown of PARP-1 has been affected, it became imperative to perform an immunophenotyping for the respective stem cell, cell signaling and pancreatic developmental markers associated with islet neogenesis. Hence, a complete profiling for all possible markers was completed using flow Cytometry. We observed a significant reduction in CD34 but rest of the CD markers viz. CD90, CD44 and CD45 in the PARP-1-KD cells remained unchanged. Further, we observed that Nestin expression was downregulated along with all the key transcription factors essential for islet differentiation viz. PDX1, NEUROG3, NEUROD, NKX6.1 and MAFA. We also screened for phosphorylated SMAD3 expression, which was again observed to have decreased in the PARP-1 KD cells (Fig 4.8).

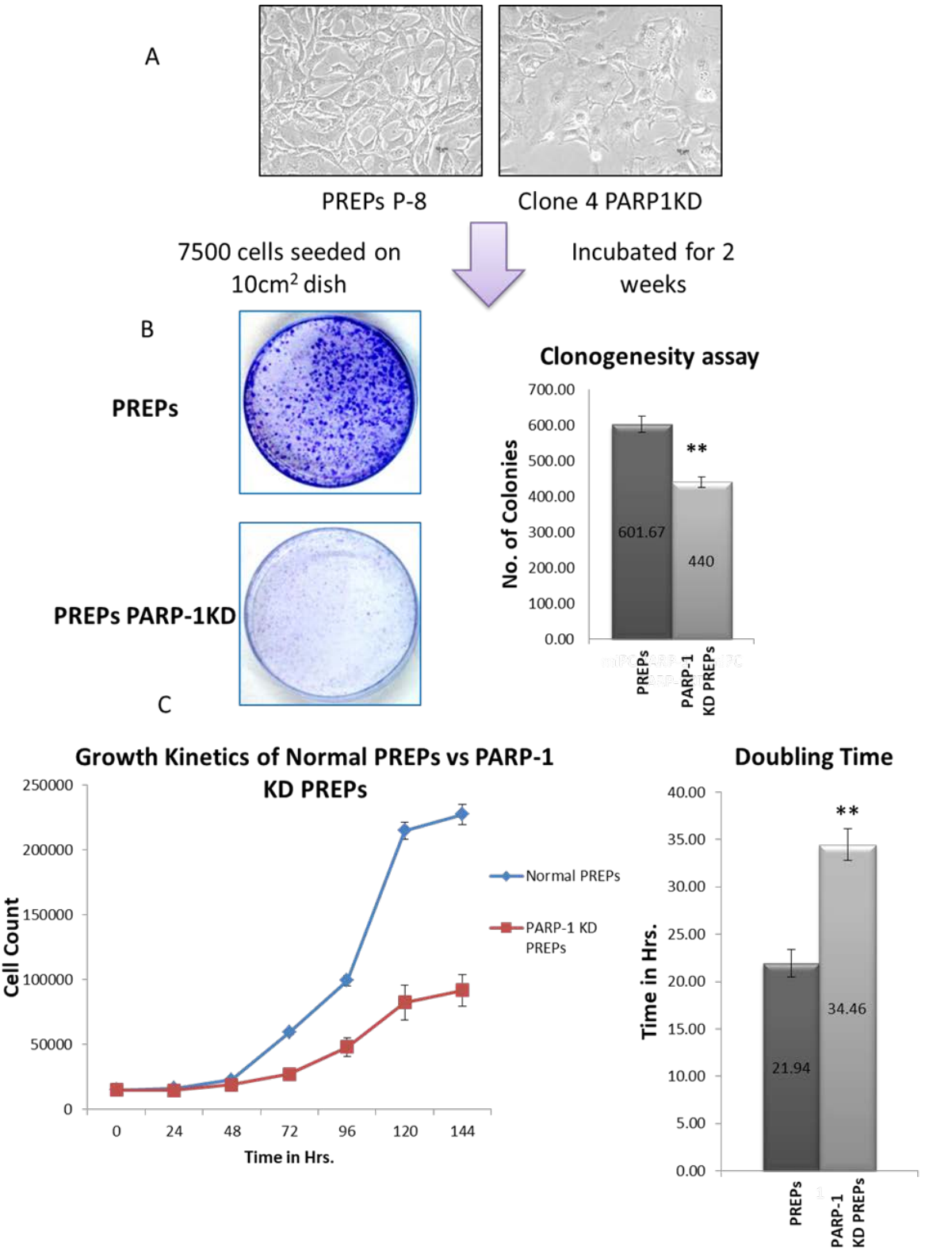

Figure 4.7: Comparative Morphology, growth kinetics and doubling time: A) Microscopic depiction of change in morphology after PARP-1 knockdown in mIPCs. B) Clonogenic assay plates to indicate loss of proliferative potential in PARP-1 knockdown cells and colony count graph where, **= p≤0.01. C) Growth kinetics plot over 144 hrs to compare the growth rate by calculating the doubling time between Normal PARP-1 & PARP-1 KD cells. **=p≤0.01. N=3.

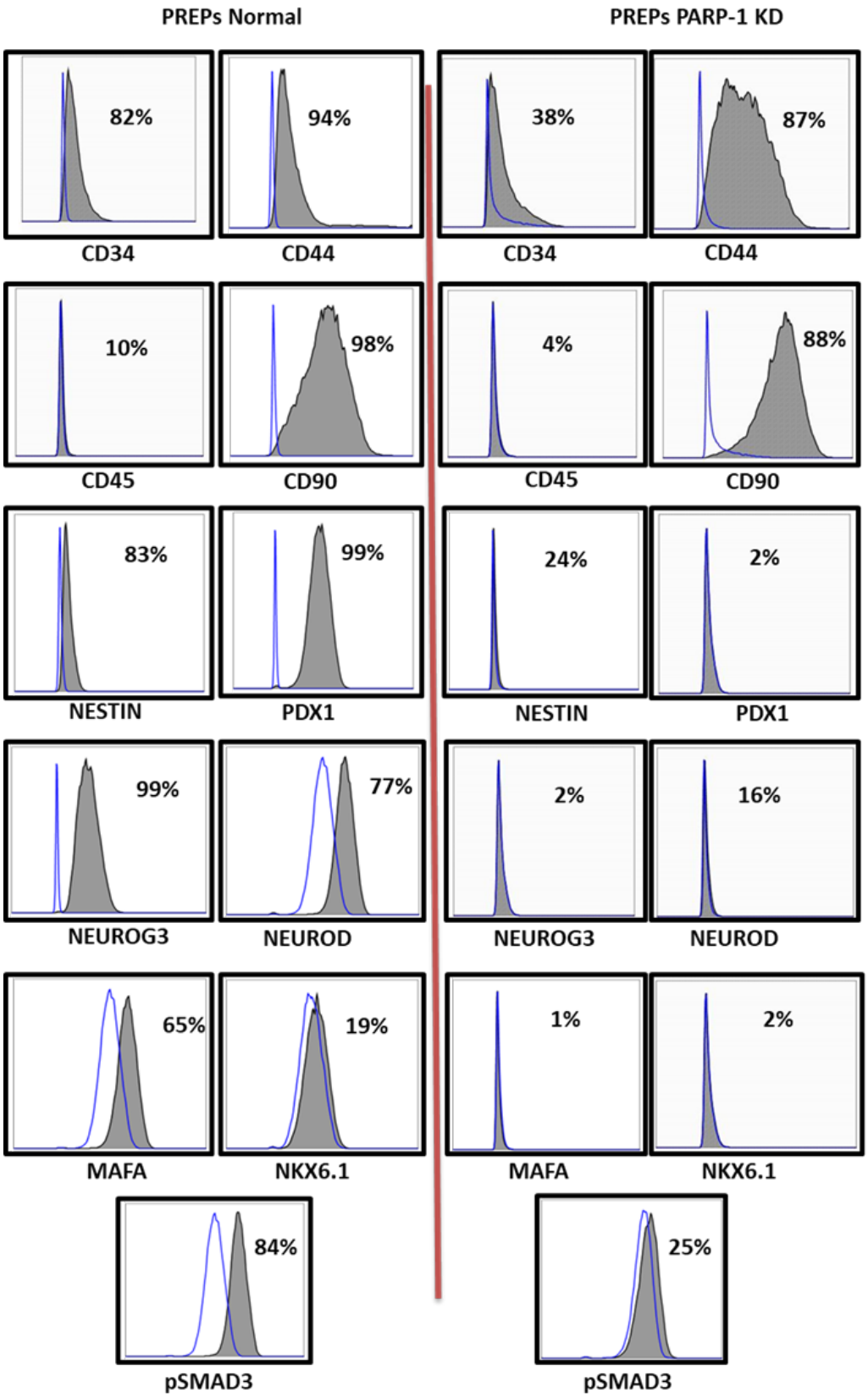

Figure 4.8: Comparative Immunophenotyping of PREPs vs PARP-1 KD PREPs: The figures demonstrate a comparative marker profile for stemness, cell signaling and pancreatic key transcription factors. N=3.

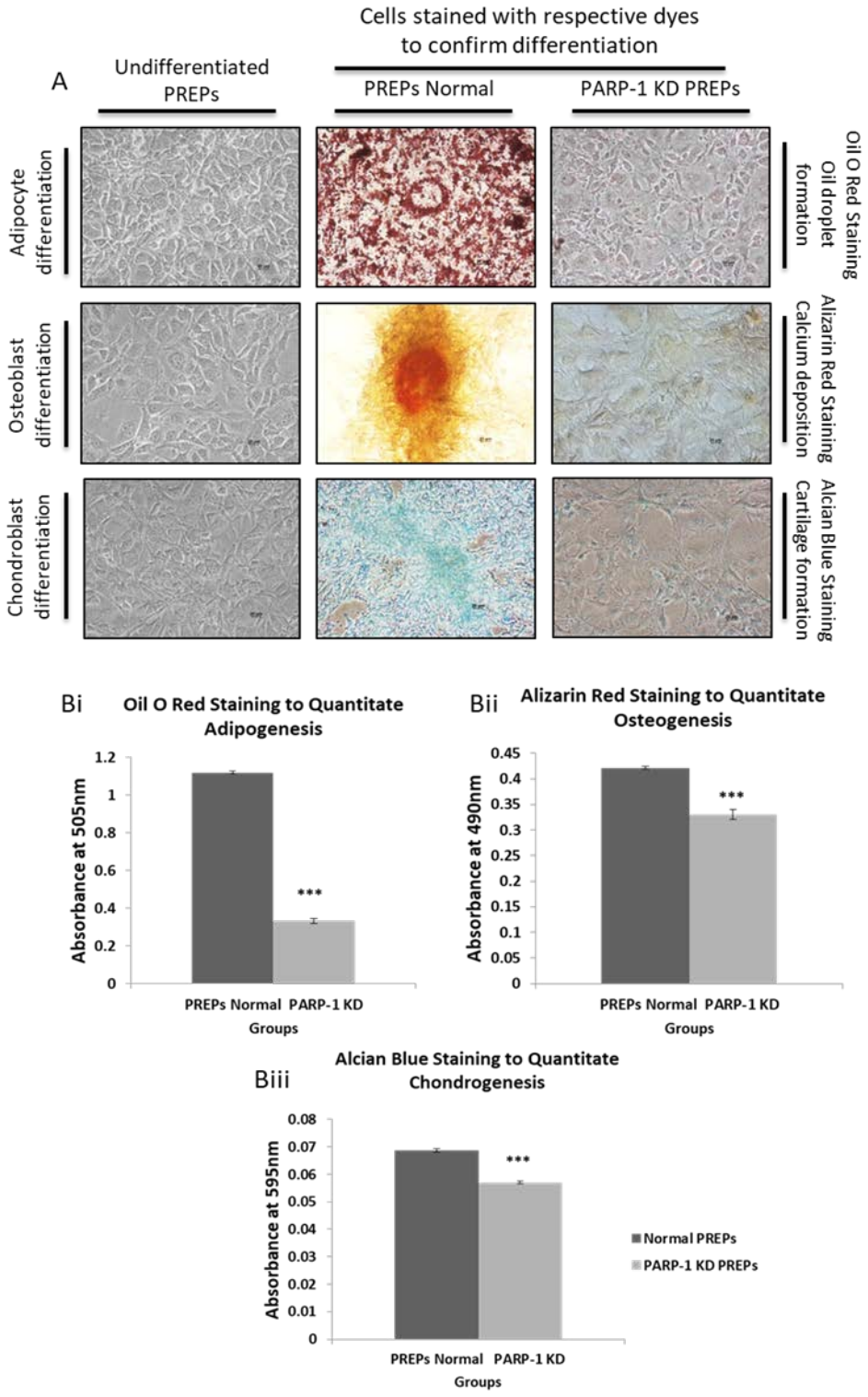

Figure 4.9: Comparative Trilineage Differentiation: (A) Trilineage differentiation of Normal PREPs & PARP-1 KD PREPs into Adipocytes, Osteoblasts and Chondroblasts respectively. Scale bar represents 20 microns (B) Quantification of differentiation (Bi) Oil O Red staining to quantify oil droplet formation; (Bii) Alizarin red staining to quantify calcium deposition and (Biii) Alcian Blue staining to quantify cartilage formation. ***=p≤0.001. N=3.

4.3.2.3. Comparative study of PARP-1 normal & KD to assess their trilineage differentiation potential:

In order to confirm that PARP-1 knockdown has abated the ability of PREPs to differentiate by moderating their stemness, we performed a trilineage differentiation study along with the PARP-1 normal cells. The results were in line with our above data where we observed that the PARP-1KD cells failed to differentiate into adipocytes, osteoblasts and chondroblasts. The differentiation was confirmed by staining with respective dyes to compare and quantify the differentiated cells. A very significant difference was observed upon their estimation between the PARP-1 normal and KD cells (Fig 4.9).

4.3.4. Standardizing the ABT888 dose for effective inhibition of PARylation while sustaining viability of PREPs:

A dose for ABT888 was selected by screening the doses from 5 nM to 5 µM for abatement of PARylation on induction with 100 µM H_2O_2 on PREPs. We observed that 5 µM dose of ABT888 completely abolished PARylation while sustaining complete viability in cells, which was observed by MTT assay (Fig 4.10).

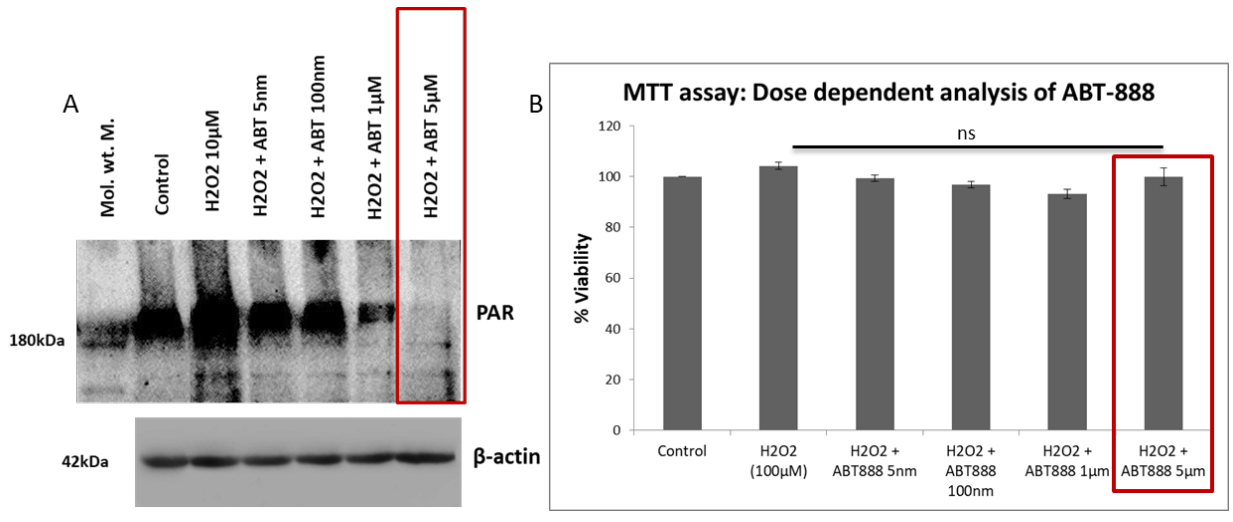

Figure 4.10: ABT888 dose standardization: (A) The figure represents inhibition of PARylation with increasing ABT888 dose. (B) The figure represent viability of cells with increasing ABT888 dose.

4.3.5. Differentiation of PARP-1normal & PARP-1KD PREPs into islet cell clusters:

PREPs PARP-1normal, PARP-1KD and PREPs treated with ABT-888(PARP-1/2 inhibitor) were differentiated into islet like cell clusters and were further functionally characterized.

4.3.5.1. Time dependent microscopic profiling was performed to observe morphological changes during Islet differentiation process:

A temporal microscopic profiling was carried out for PARP-1normal, PARP-1KD and ABT-888 treated cells to assess the rate and extent of differentiation, where Islet differentiation for the PARP-1KD cells was observed to have subsided very significantly compared to the other two groups. We observed that the PARP-1 KD cells failed to form clusters by migrating towards a central point and maturing instead they were found be adhered to the culturing surface. Also, DTZ staining of the islet clusters were performed to confirm presence of Insulin within the clusters and again it turned out negative in the PARP-1KD cells which was to be expected for the poor cluster formation. There was no significant change observed in the ABT-888 treated group from the Normal control group suggesting PARP-1 regulatory role being independent of its enzyme activity (Fig 4.11).

4.3.5.2. Functional assessment of islet cell clusters across the groups by Immunocytochemistry and C-peptide release assay by ELISA:

The differentiated islets like cell clusters were further functionally characterized by immunocytochemistry for PARP-1, Nkx6.1, C-Peptide and Glucagon. Proportional change in their expression was observed i.e. no expression of Nkx6.1, C-peptide or glucagon was observed in the PARP-1KD PREPs, whereas there was no change observed in the ABT-888 treated group from the control group of PARP-1normal PREPs (Fig 4.12). Further, c-peptide release against glucose challenge demonstrated a significant decrease in the PARP-1 KD groups in both Activin and Swertisin differentiated islets, whereas there was no difference

between the PARP-1 Normal control islets and ABT888 treated islets in either groups (Fig 4.13).

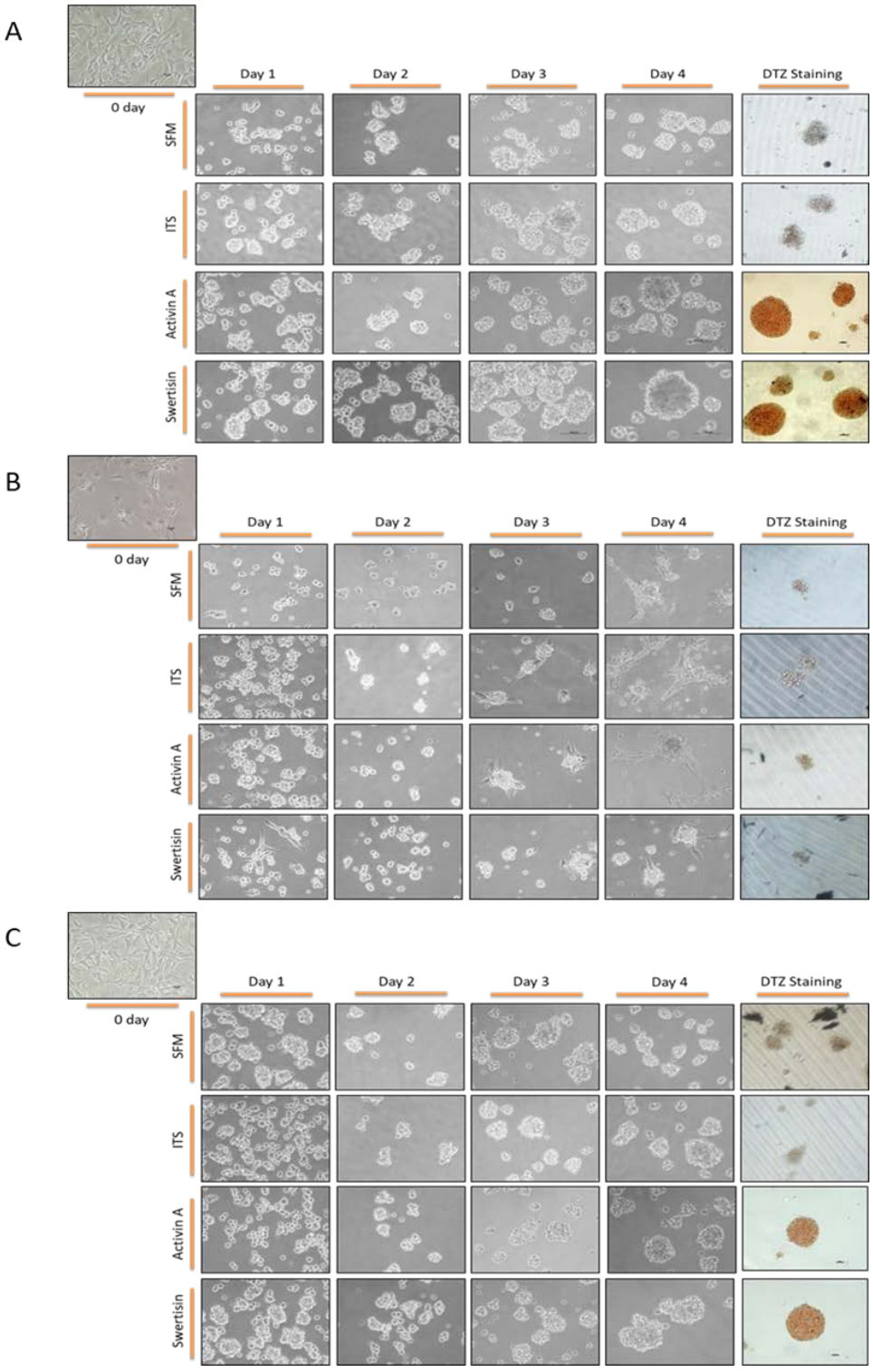

Figure 4.11: Comparative Islet Differentiation: Fig A,B &C represents temporal microscopic Islet differentiation profile through 4 days of differentiation in PREPs, PARP-1 KD PREPs and PREPs treated with ABT-888 (PARP-1 specific inhibitor) respectively. It is observed that islet cluster formation is abolished in PARP-1 knock down cells but not in the ABT-888 treated cells. Scale bar represents 100 microns.

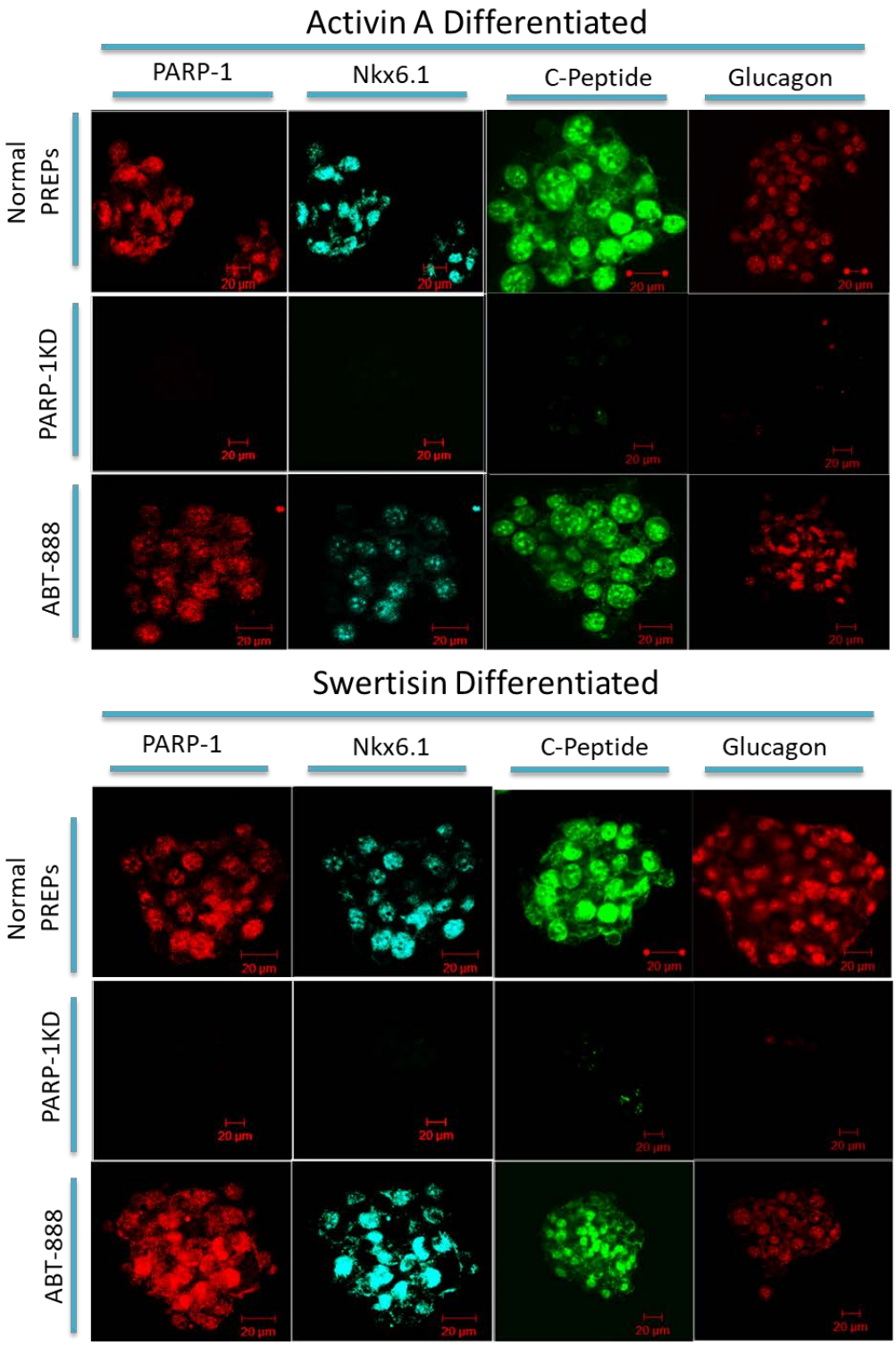

Figure 4.12: Functional Assessment of PREPs, PARP-1 KD PREPs and ABT888 treated PREPs: PARP-1 knock down cells do not differentiate into islets and are negative for PARP-1(red), NKX6.1 (cyan), c-peptide (green) and glucagon (red) compared to normal PREPs and ABT888 treated cells which produce islet clusters positive for the above markers. Scale bar represents 20 microns.

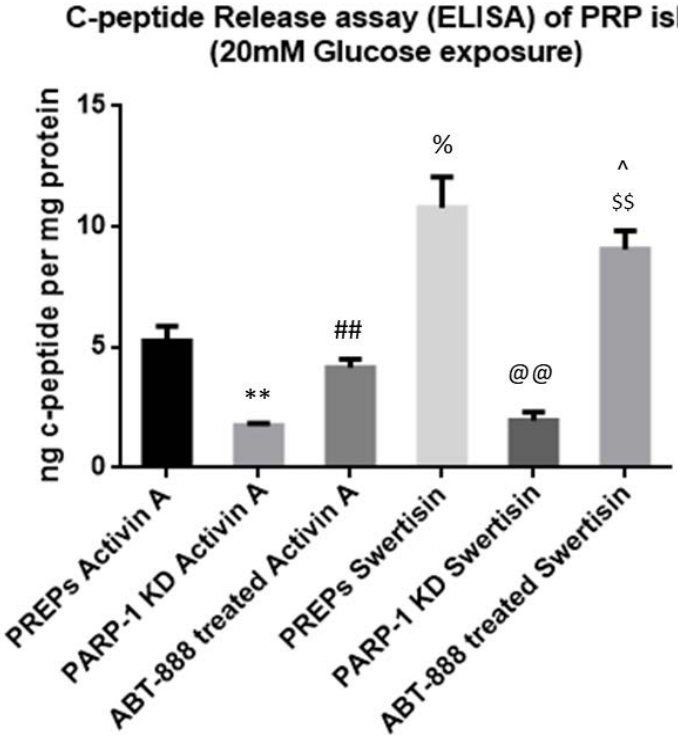

Figure 4.13: Functional Assessment of PREPs, PARP-1 KD PREPs and ABT888 treated PREPs: The graph represents comparative c-peptide release in response to glucose challenge. The graphs were plotted with Mean ± SEM. **=p≤0.01 PREPs Activin A vs PARP-1 KD Activin A; ##=p≤0.01 PARP-1 KD Activin A vs ABT-888 treated Activin A; %=p≤0.05 PREPs Activin A vs PREPs Swertisin; @@=p≤0.01 PREPs Swertisin vs PARP-1 KD Swertisin and $$=p≤0.01 PARP-1 KD Swertisin vs ABT-888 treated Swertisin. ^ =p≤0.05 ABT-888 treated Activin A vs ABT-888 treated Swertisin. N=3.

4.3.6. Comparative temporal protein profile of PARP-1 normal and stable PARP-1 knock down PREPs clone 4:

Western blots showed no PARP-1 expression in the PARP-1 KD panel which was to be expected as the clone was a stable knockdown. Further we also observed reduced PARylation compared to the PARP-1 normal panel. Nestin persisted throughout PARP-1 knock down cells which confirms their inability or abatement of islet differentiation. Phosphorylated SMAD3 expression was heavily downregulated in the PARP-1 KD panel. Time dependent protein expression demonstrated a down regulation of pancreatic developmental markers like PDX1 NEUROG3, NEUROD, PAX4, NKX6.1 and MAFA which are paramount for islet differentiation and homeostasis. Beta actin was used as an endogenous control (Fig 4.14).

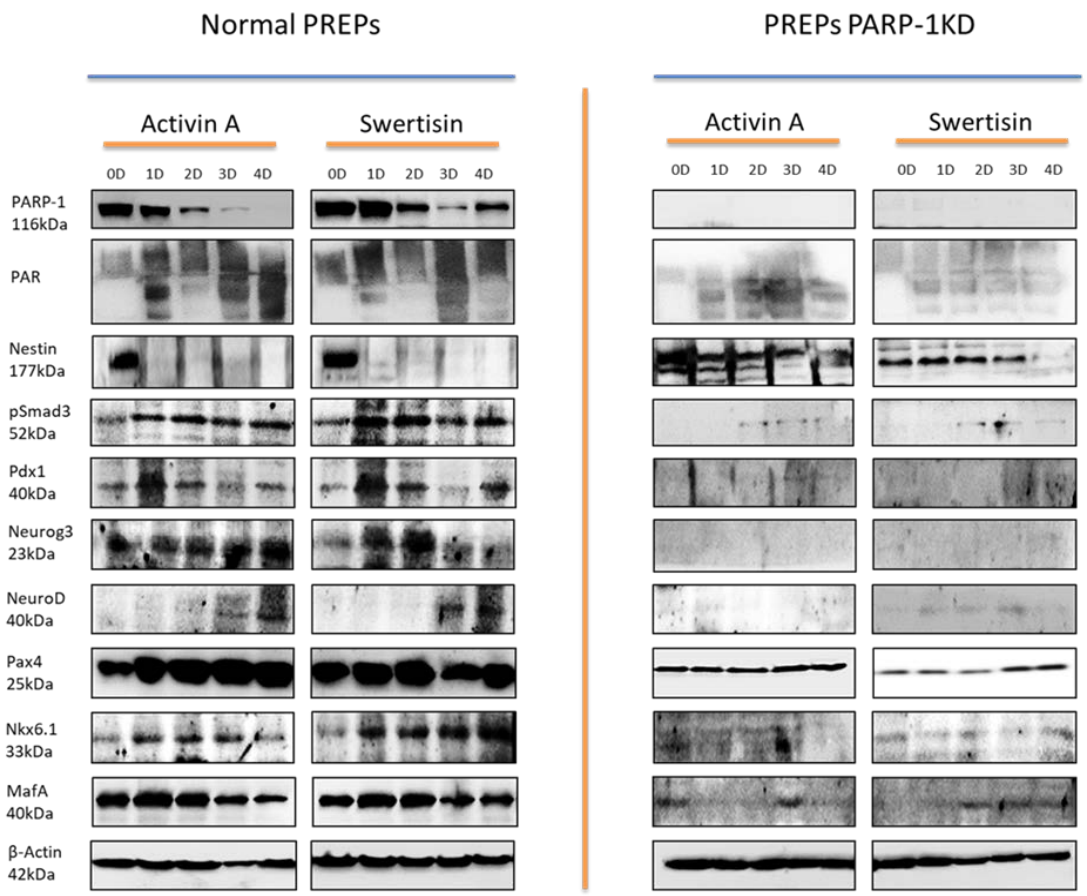

Figure 4.14: Temporal protein profiling between Normal PREPs and PARP-1 KD PREPs during islet differentiation: The figure demonstrates comparative protein profiling indicating downregulation of several key transcription factors associated with islet differentiation in PARP-1 KD PREPs. N=3.

4.3.7. Confirming the PARP-1 KD phenotype and the above results in islet differentiation from PREPs by using siRNA:

We confirmed the above results by treating PREPs with siRNA specific for PARP-1 gene which had the same sequence as the one in the pSIP912 vector. We confirmed PARP-1 knockdown by western blotting where b-actin served as endogenous control. We observed abatement of islet cluster formation on subjecting these cells to islet differentiation inducing from both Activin A and Swertisin. Functional characterization of these cells demonstrated highly reduced expression of both c-peptide (yellow) and Nkx6.1 (green) suggesting that PREPs couldn't terminally differentiate into mature beta cells (Fig 4.15).

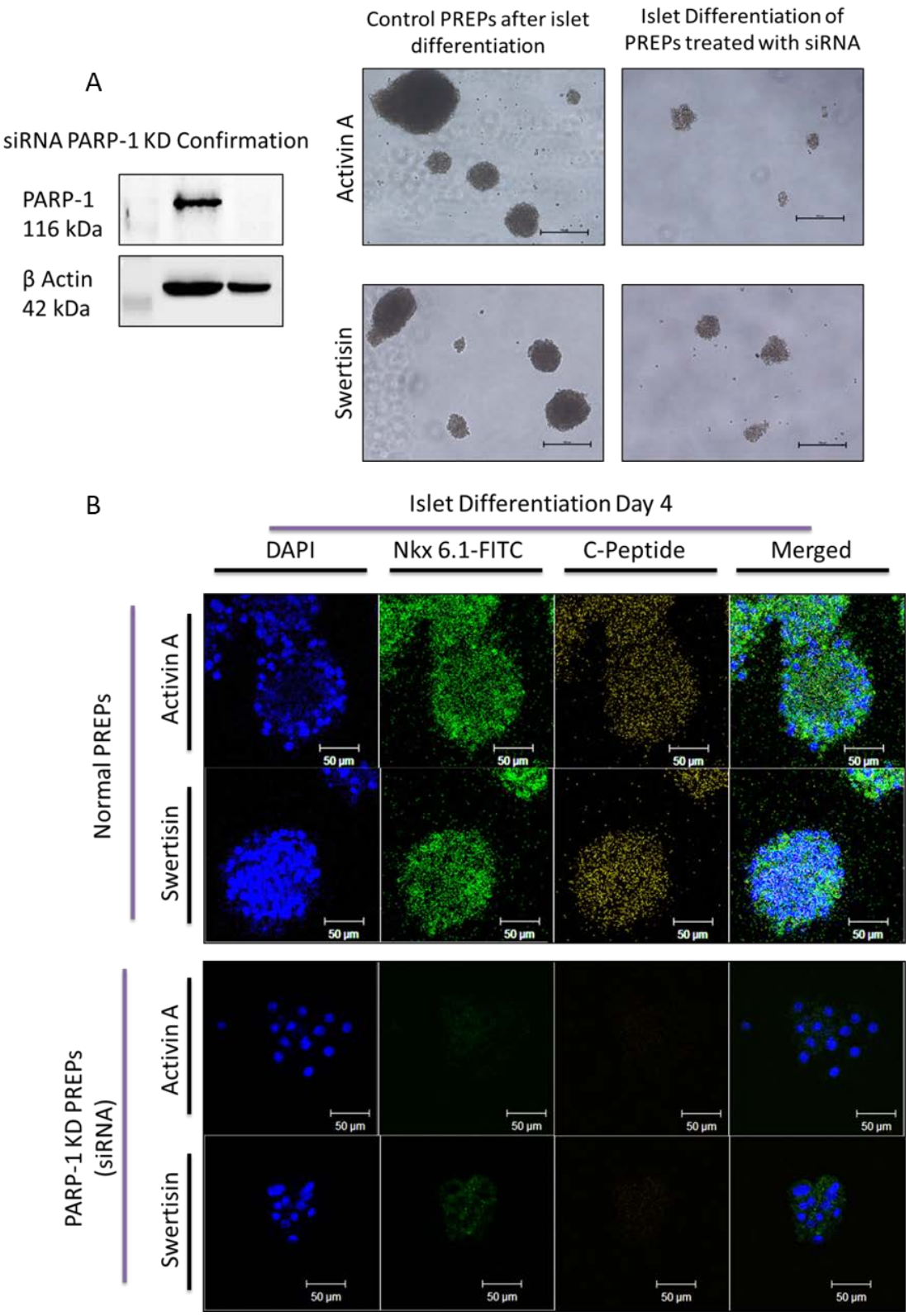

Figure 4.15: Confirmation of PARP-1 KD phenotype in islet differentiation by using siRNA against PARP-1: (A) The figure represents confirmation of PARP-1 knockdown by western blotting and abatement of islet cluster formation in siRNA treated PREPs. (B) Comparative Functional characterization of islet clusters in Normal PREPs and siRNA treated PREPs. Scale bar represents 50 microns.

4.3.8. PARP-1 recovery inducing regain of islet differentiation potential of PREPs by reintroducing PARP-1 in knockdown PREPs using recovery vector to confirm the role of PARP-1 in islet differentiation:

In order to confirm and establish that PARP-1 is vital for islet differentiation we recovered PARP-1 protein by transfecting a recovery vector resistant to PARP-1 silencing in PARP-1 KD PREPs. We confirmed the recovery of PARP-1 by western blotting. These cells were then differentiated into islet like cell clusters. We observed formation of islet clusters same as that of control PREPs and were positive for DTZ staining suggesting presence of Insulin within these clusters. This was confirmed by immunocytochemistry where the recovered islets were positive for both c-peptide and glucagon. Further, C-peptide release assay against glucose challenge confirmed the functionality of the recovered islets as there was a significant increase in the c-peptide release in the PARP-1 recovered islets when compared to the PARP-1 KD islets in both Activin A and Swertisin groups (Fig 4.16 & 4.17).

4.3.9. Confirming the above hypothesis in PANC-1 cells, which serves as a human pancreatic progenitor model system:

The hypothesis of PARP-1's role in islet neogenesis was culminated from our lab previous study where it was observed that PARP-1 knockdown in the PANC-1 cells lead to complete abolishment of islet formation (Nidheesh Dadheech thesis, 2013). Hence in order to augment and support our above data and observe molecular changes we subjected PANC-1 U6 (empty vector) cells and PANC-1 Sip (PARP-1 KD) cells to islet differentiation. We observed similar results as in PREPs and observed complete abatement of islet cluster formation. We further harvested these cells at day5 (midpoint) of a ten day differentiation process and performed a transcriptome and protein analysis by taqman gene array and western blotting respectively. We observed key transcription factors in islet differentiation were significantly downregulated indicating abatement of islet differentiation as observed phenotypically which were in line with our above data of PREPs (Fig 4.18).

Figure 4.16: Recovery of PARP-1 in the PARP-1 KD PREPs: (A) The figure demonstrates confirmation of PARP-1 after introduction of recovery vector in PARP-1 KD PREPs. (B) represents temporal microscopic Islet differentiation profile through 4 days of differentiation in PREPs, PARP-1 KD PREPs and PARP-1 recovered PREPs. Scale bar represents 100 microns. N=3.

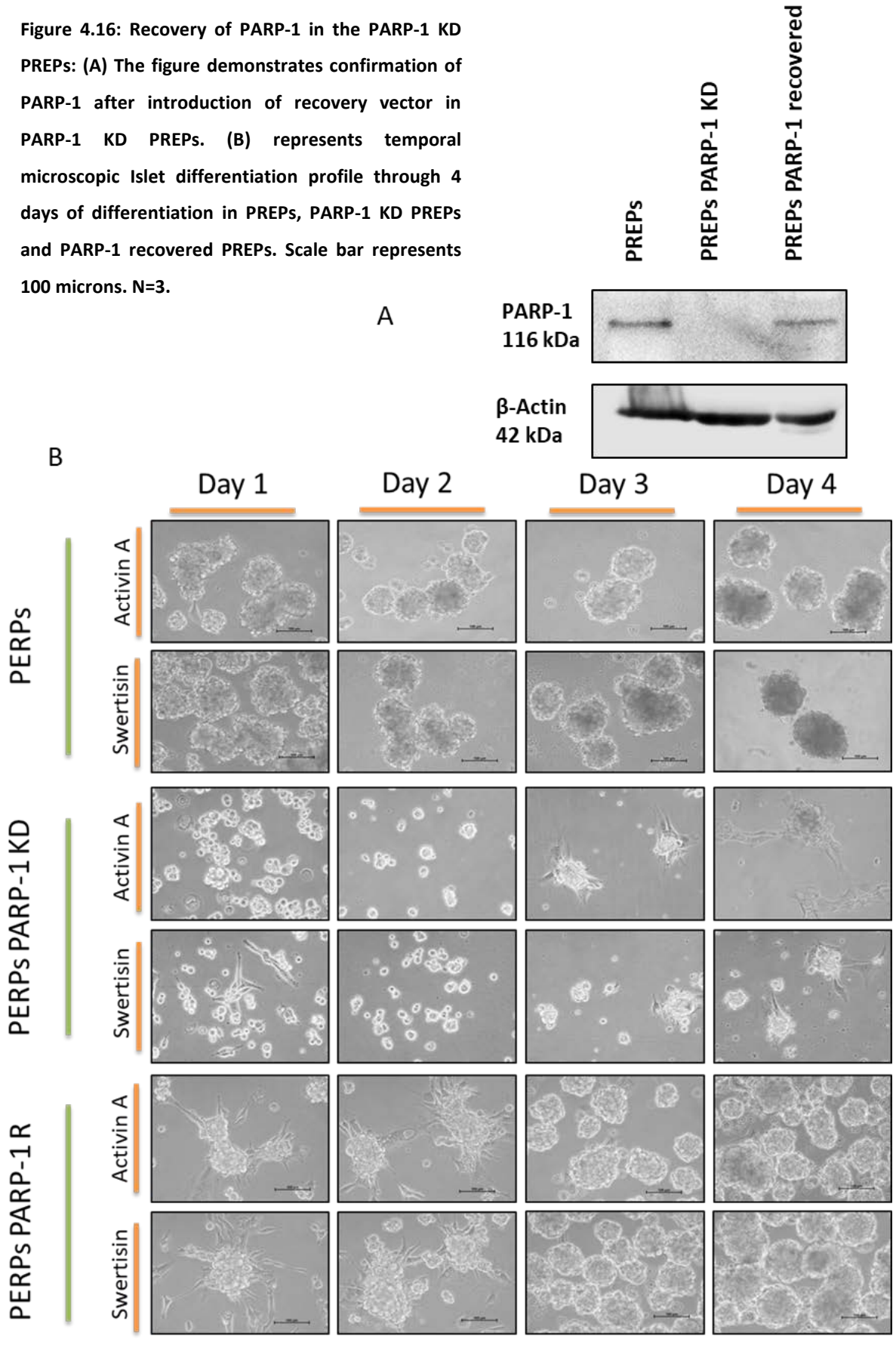

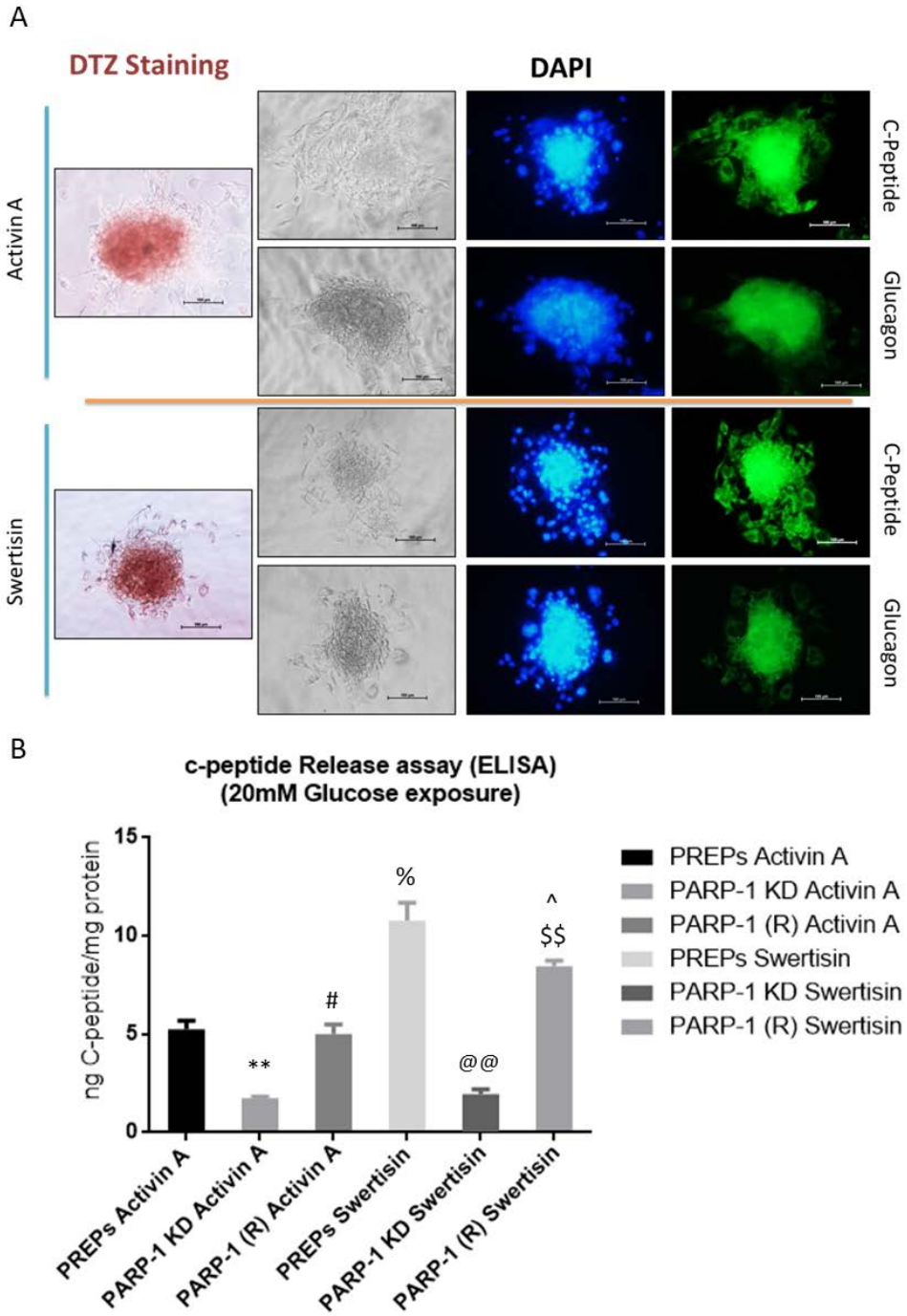

Figure 4.17: Functional characterization of islets post PARP-1 recovery: (A) The figure represents functional assessment of islets after PARP-1 recovery by immunocytochemistry. Scale bar represents 100 microns. (B) The graph represents comparative c-peptide release in response to glucose challenge. The graphs were plotted with Mean ± SEM. **=p≤0.01 PREPs Activin A vs PARP-1 KD Activin A; #=p≤0.05 PARP-1 KD Activin A vs PARP-1 (R) Activin A; %=p≤0.05 PREPs Activin A vs PREPs Swertisin; @@=p≤0.01 PREPs Swertisin vs PARP-1 KD Swertisin and $$=p≤0.01 PARP-1 KD Swertisin vs PARP-1 (R) Swertisin. ^ =p≤0.05 PARP-1 (R) Activin A vs PARP-1 (R) Swertisin. N=3.

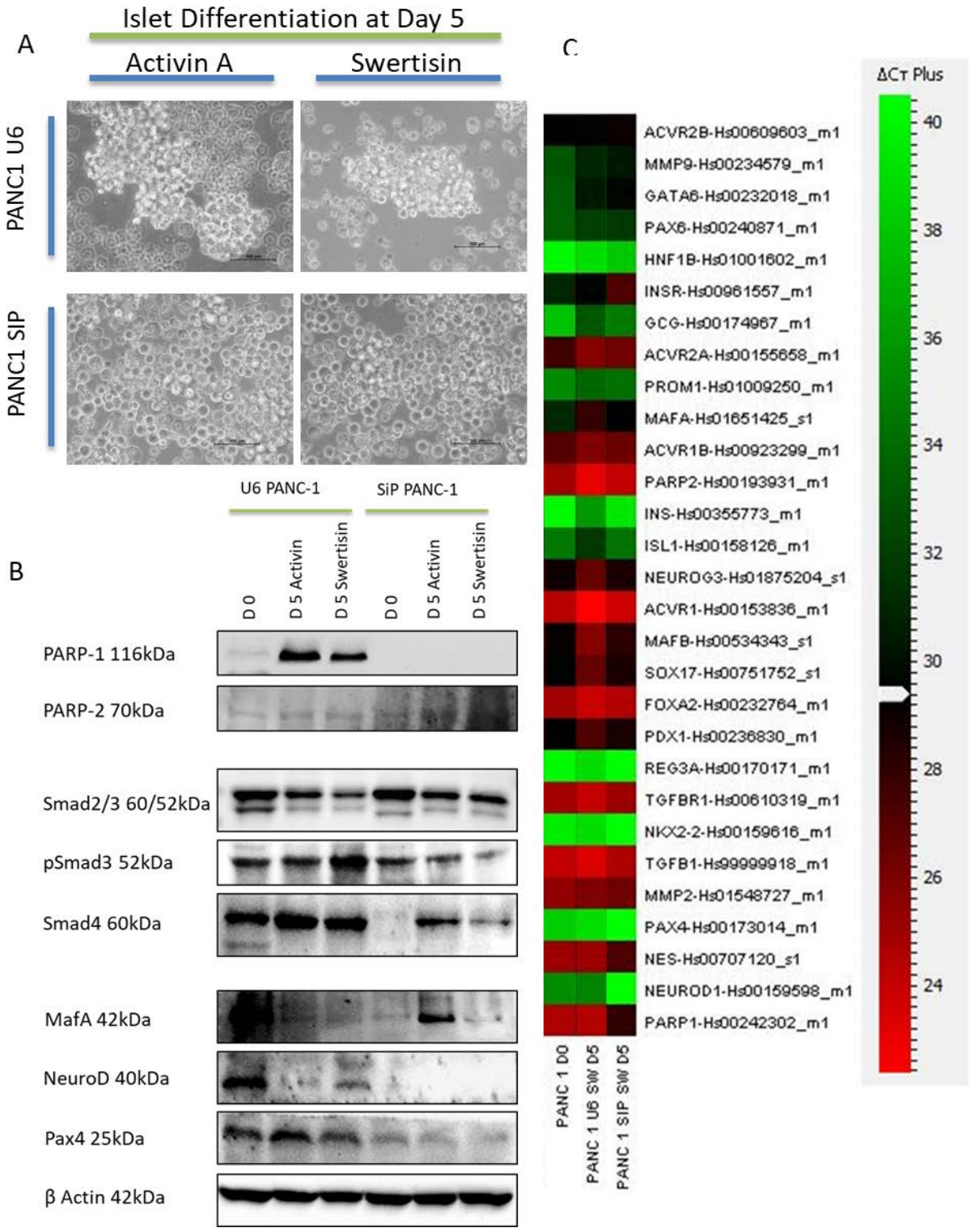

Figure 4.18: Confirming Role of PARP-1 in islet differentiation from PANC-1 cells: (A) The figure shows abatement of islet differentiation at day 5 in PANC-1Sip cells post PARP-1 knockdown. Scale bar represents 100 microns. (B) Comparative protein profiling between PANC1U6 and PANC1 SiP cells at 5th day of islet differentiation in both Activin A and Swertisin groups. (C) The figure demonstrates a gene array data which shows down regulation of all the important pancreatic genes post PARP-1 knockdown (Green-lowest to Red-Highest). N=3.

4.3.10. Phosphorylation of Smad3 is essential for islet differentiation:

Many reports suggest TGF-β SMAD signaling is central to the paradigm of islet differentiation. In our previous lab reports we have discussed that both Activin A and Swertisin follow this pathway where activation of Smad3 becomes vital. Here in our above data we have observed that during islet differentiation phosphorylation of SMAD3 increases. Hence in order to confirm the importance of Smad activation in islet differentiation we used SIS3, which inhibits phosphorylation of SMAD3. We observed absolute abolishment of islet cluster formation with respect to that of the control PREPs. This confirms that SMAD3 activation and signaling is paramount in islet differentiation (Fig 4.19).

4.3.11. Nuclear localization of activated SMADs during islet differentiation:

In TGF-β SMAD signaling as described in chapter 1 of the thesis, upon activation a complex of pSMAD2, pSMAD3 and SMAD4 is formed which translocate within the nucleus and regulates the expression of specific target genes. We confirmed this phenomenon by immunocytochemistry and fractionating the cytoplasmic and nuclear fractions to observe presence of phosphorylated SMAD3. In the undifferentiated PREPs pSMAD3 expression was observed completely in the cytoplasm however in the mature islets the pSMAD3 has localized within the nucleus. This was confirmed by fractionation, where we observe similar phenomenon, where pSMAD3 and SMAD4 were present robustly within the nuclear fraction during islet differentiation as compared to the undifferentiated cells where they remained in the cytoplasmic fraction (Fig 4.20).

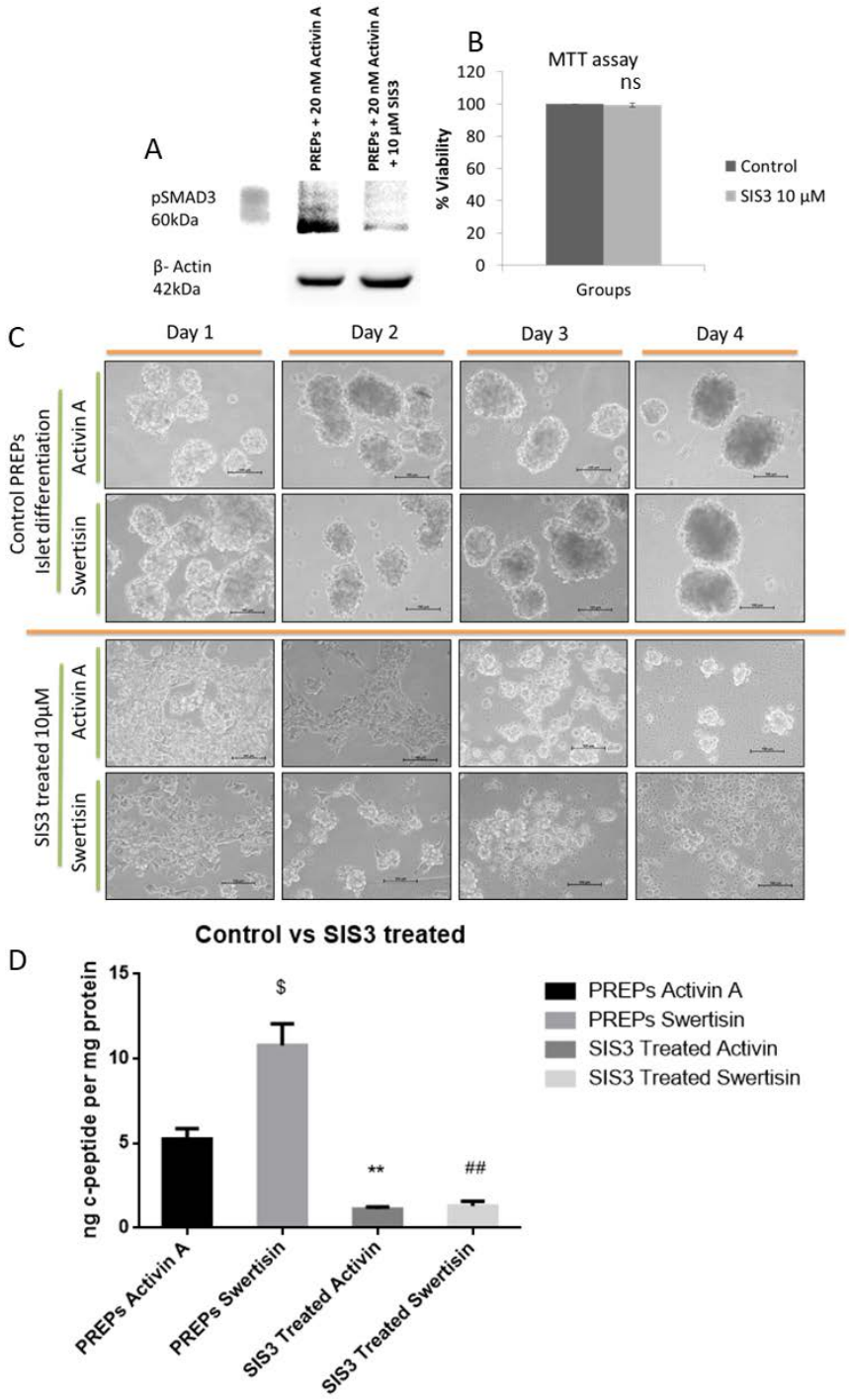

Figure 4.19: Effect of SIS3 on islet differentiation: (A) The figure shows abatement of islet differentiation at day 5 in PANC-1Sip cells post PARP-1 knockdown. Scale bar represents 100 microns. (B) Comparative protein profiling between PANC1U6 and PANC1 SiP cells at 5th day of islet differentiation in both Activin A and Swertisin groups. (C) The figure demonstrates a gene array data which shows down regulation of all the important pancreatic genes post PARP-1 knockdown (Green-lowest to Red-Highest). (D) c-peptide release assay with control and SIS3 treated groups. $= p≤0.05 PREPs Activin A vs PREPs Swertisin; ** p≤0.01 PREPs Activin A vs SIS3 Activin A; ## p≤0.01 PREPs Swertisin vs SIS3 Swertisin. N=3.

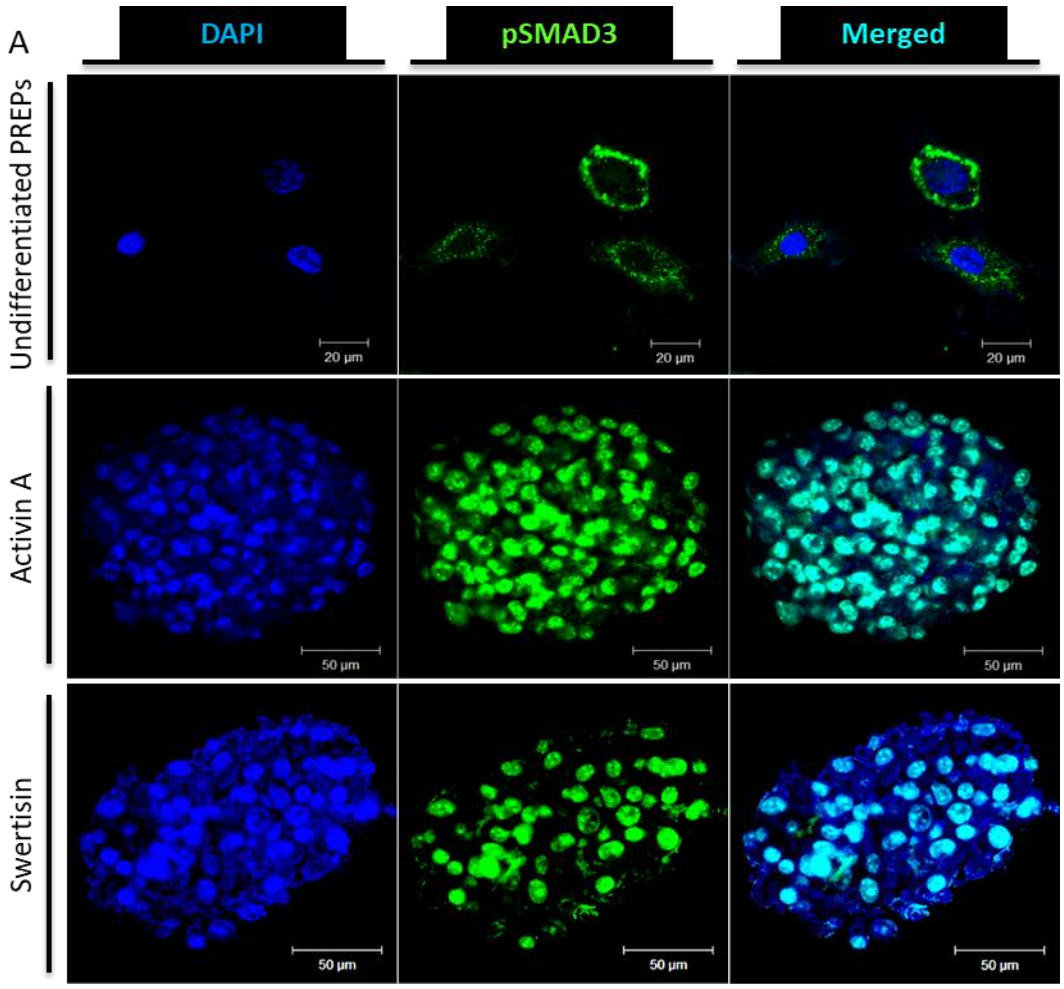

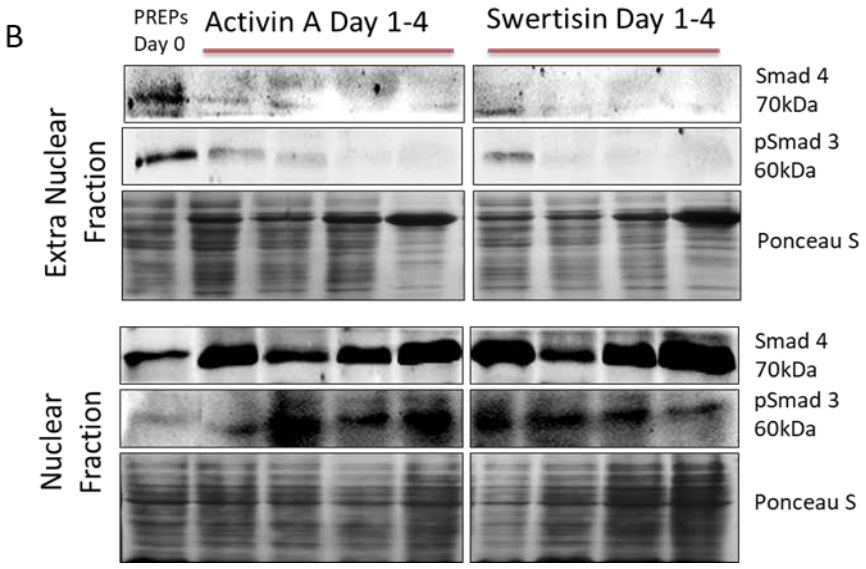

Figure 4.20: Localization of pSMAD3 and Smad4 during islet differentiation from PREPs: (A) Immunocytochemistry of undifferentiated and differentiated PREPs to demonstrate pSMAD3 (green) localization. (B) Fractionation study during islet differentiation from PREPs to confirm localization of pSMAD3 and SMAD4 in the nuclear fraction.

4.3.12. Interaction of PARP-1 with SMADs:

As described in chapter 1 there have been reports where PARP-1 interacts with SMADs and regulate the signaling cascade within the nucleus. PARP-1 being a nuclear protein, we also wanted to explore the possibility of PARP-1 and Smad interaction. Also, from our temporal protein profiling in during islet differentiation from both PREP and PANC-1 cells it was observed that phosphorylation of Smad3 was downregulated. Hence, In order to understand the signaling mechanism of PARP-1 in islet differentiation and based on the gene and protein profile data we performed Co-Immunoprecipitation of PARP-1 on day 4 of the PREPs and day 5 of the PANC-1 islet differentiation. We observed a robust interaction of PARP-1 with the TGF-β signaling molecules of Smad3 and pSmad3. We observed that as differentiation progressed the interaction of PARP-1:SMAD3 goes down whereas the interaction of PARP-1:pSMAD3 increased which propelled islet differentiation (Fig 4.21).

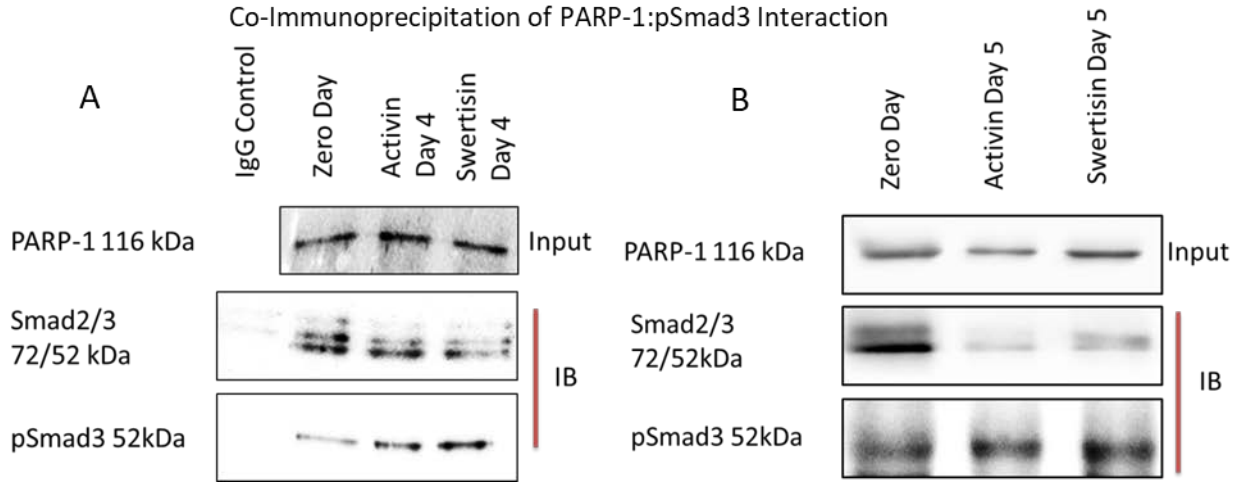

Figure 4.21: PARP-1 Co-IP: (A) The figure demonstrates IP of PARP-1 at 4th day of PREPs differentiation where PARP-1:Smads interaction is observed. (B) The figure demonstrates PARP-1:Smad Interaction at day 5 of islet differentiation in PANC-1 cells.

4.3.13. Chromatin Immunoprecipitation of PARP-1during islet differentiation to confirm its gene regulatory function:

The above data from both PREPs and PANC-1 cells strongly suggested that PARP-1 depletion modulated the expression of key transcription factors essential for islet differentiation. We performed a chromatin Immunoprecipitation with PARP-1 antibody and identified the promoter regions of key transcription factors with which PARP-1 protein demonstrated interaction. We observed that the most strong interaction was between Neurog3 gene promoter site (55 to 71) bases downstream of transcription start site (TSS) present in the first exon region in both Activin A and Swertisin groups. We also observed PARP-1 interaction at other key transcription factor promoter sites during islet differentiation viz. Reg3a (-83 to -67) upstream of TSS; Pdx-1 (-207 to -191) upstream of TSS; Neurog3 (55 to 71) downstream of TSS; NeuroD (-39 to -16) upstream of TSS; Pax4 (-401 to -385) and Nkx6.1 (21 to 37) downstream of TSS.

This data confirmed that PARP-1 positively regulates the key transcription factors during islet differentiation by significantly increasing its interaction at the promoter regions of these transcription factors and positively modulating them during islet differentiation from PREPs (Fig 4.22).

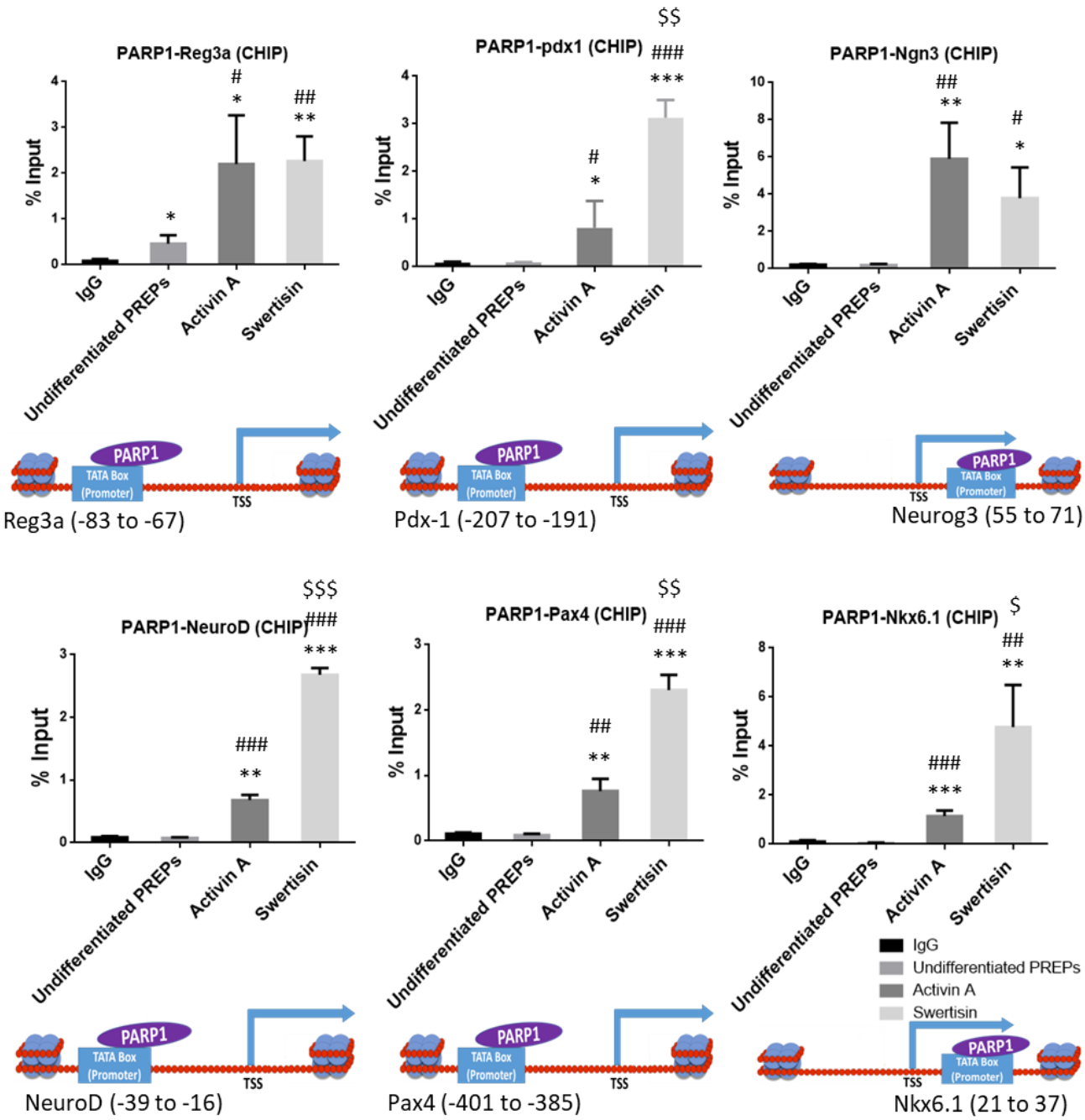

Figure 4.22: CHIP:PARP-1 in islet differentiation from PREPs: The figure demonstrates interaction of PARP-1 with the promoter regions of the key transcription factors during islet differentiation. The graph plotted is MEAN ± SEM. */#/$=p≤0.05; **/##/$$=p≤0.01 and ***/###/$$$=p≤0.001. *vsIgG; #vsUndifferentiated PREPs; $vsActivinA.

4.4. Discussion

PARP-1 is a ubiquitous nuclear protein present in all tissues of eukaryotes except yeast. Relative expression of PARP-1 in all the tissues identifies that its expression in the pancreas is significantly lower than any other tissue/organ which indicates that PARP-1 has a profound unique and very tightly regulated role within the pancreas (Fagerberg et al., 2014). In present study we aimed to explore PARP-1's regulatory role in the paradigm of islet differentiation from stem/progenitors and identify its gene targets to help us expand our understanding of both PARP-1's transcription control potential and its significance in generating new islets. This study has been performed with mouse primary pancreatic progenitors (PREPs) and supported by PANC-1 cells, which is a cell line model for human pancreatic progenitors.

PARP-1 gene was silenced in both the cell types by using shRNA vectors. pSIP912 do not have either a reporter nor a selection marker, hence pEGFP-N1 was co-transfected with pSIP912 in PREPs, which had a neomycin selection gene and GFP reporter. PANC-1 cells both pUBSU6 (empty vector) and pSIP912 cells (having PARP-1 shRNA) were previously generated in the lab. (Dr. Nidheesh Dadheech Thesis, 2013).

We observed morphological changes after PARP-1 depletion in PREPs. This could be as PARP-1 is a ubiquitous protein involved in a plethora of regulatory mechanisms. The PARP-1 KD PREPs has a significantly low growth rate which was evident by the Clonogenic assay and growth kinetics as compared to normal PREPs .In the KD group we observed very few and smaller colonies with significantly increased doubling time. PARP-1 has been previously implicated in regulating cell growth as it acts as a negative regulator of FOXO1, which mediates the expression of cell cycle inhibitor p27. Hence, with PARP-1 depletion FOXO1 gains function thereby decreasing cell proliferation (Sakamaki et al., 2009). In a more recent report PARP-1 inhibition decreases the PARylation of Sp1, a transcription factor involved in activation of G0/G1 phase genes, thereby arresting cells in the G0/G1 phase and decreasing their proliferation (Yang et al., 2013).

As these cells demonstrated deviation from their normal morphology and growth kinetics, it became imperative to characterize these cells again. The comparative immunophenotyping showed certain

interesting differences in the marker profile of both Normal PREPs and PARP-1 KD PREPs. We observed there were no significant changes in the CD marker profile of MSCs except for CD34. CD34 expression was significantly downregulated. CD34 has been identified as a marker present in tissue specific progenitors (Sidney et al., 2014). Nestin, a signature marker for pancreatic progenitors was down regulated post PARP-1 KD indicating that PARP-1 KD PREPs might have lost their pancreatic progenitor identity (Afelik and Rovira, 2017; Kim and Hebrok, 2001a; Zhang et al., 2005). Hence, we further characterized these cells to understand aberrations in their differentiation potential. A comparative trilineage differentiation between normal PREPs and PARP-1 KD PREPs demonstrated a complete abolishment of PARP-1 KD PREPs differentiation potential and thus losing their multipotency. There was no differentiation observed in Adipocyte, Osteocyte or Chondrocyte differentiation. It has been reported that PARP-1 is essential in embryonic stem cells to maintain pluripotency as its depletion results in alteration in the expression of genes that regulate metabolism, signal transduction and cell cycle (Ogino et al., 2007). Further, PARP-1 has been reported to interact with pluripotency markers like Oct4 and Sox2. It has been demonstrated that PARP-1 directly interacts with Sox2 which then activates Fgf4, an essential step in cellular reprogramming (Gao et al., 2009; Pardo et al., 2010). Also, there are other reports that PJ34 a potent PARP inhibitor can suppress Osteogenic differentiation from MSCs (Kishi et al., 2015).

We further performed islet differentiation with normal PREPs, PARP-1 KD PREPs and PREPs treated with ABT-888, a PARP-1/2/3 specific inhibitor (Kotz, 2012). In doing so we addressed whether PARP-1 enzyme activity is a prerequisite for islet differentiation. We observed successful islet differentiation from PREPs and PREPs treated with ABT-888. However, as expected from above results the PARP-1 KD cells that had lost their pancreatic progenitor characteristics and differentiation potential did not differentiate into functional islet clusters. Our earlier lab studies have shown similar data in PANC-1 cells with PJ34 PARP inhibitor (Dr. Nidheesh Dadheech Thesis, 2013). Islet maturation and functionality was confirmed by DTZ staining, immunocytochemistry for c-peptide, NKX6.1, glucagon and PARP-1 was performed across the groups from both Activin A and Swertisin generated islets. There was no difference in functionality of PREPs and PREPs treated with

ABT-888 suggesting that inhibition of PARP-1/2/3 activity alone does not hamper islet differentiation.. In other words, PARP-1's interactions with proteins or its regulatory action with transcription factors during islet neogenesis is believed to be independent of its enzyme activity. There have been a few previous reports where PARP-1 acts directly as a coactivator of NF-KB by binding to both its subunits and enhance gene expression independent of PARP-1 DNA binding and enzyme activity (Hassa et al., 2001). In a similar report it was verified that PARP-1 binds to E2F-1 which enhances its binding to its promoter thus acting as a positive cofactor of E2F-1- mediated transcription which was independent of PARP-1 DNA binding or enzyme activity (Simbulan-Rosenthal et al., 2003). Similar function was observed for Retinoic acid receptor mediated transcription where a mechanism of PARP-1 as a switch for transcriptional activation has been described, which is independent of its enzyme activity (Pavri et al., 2005).

A temporal protein profiling was performed comparing the normal PREPs and the PARP-1 KD PREPs to identify possible key targets of PARP-1 which regulate islet differentiation from progenitors. We observed reduced PARylation in the PARP-1 KD groups, the residual PARylation could be due to the activity of the other PARP proteins in the PARP family. Nestin is a classical pancreatic progenitor marker which is seen to decrease with the progression of islet differentiation (Kim et al., 2010). In the PARP-1 KD groups we observe persistent expression of Nestin throughout the islet differentiation which suggests the inability of PREPs to transition from its progenitor state to a terminally differentiated islet cluster formation.

In the PARP-1 KD groups reduced expression of phosphorylated SMAD3 was also observed which is necessary in the TGF-β mediated SMAD signalling during islet differentiation (Brown and Schneyer, 2010; Kim and Hebrok, 2001b). Also, all the key transcription factors viz. PDX-1, NEUROG3, NEUROD, PAX4, MAFA and NKX6.1 were all heavily downregulated in the PARP-1 KD groups during islet differentiation. It is well known that their sequential and timely expression is paramount for islet differentiation and function (Cerf, 2006). We also observed similar results on characterization of undifferentiated PARP-1 KD PREPs with flowcytometry compared to the normal PREPs that their inherent expression of pSMAD3 and the expression of key pancreatic developmental transcription

factors were significantly suppressed. Therefore, as all these key transcription factors were downregulated in PARP-1 KD groups there was abolishment of islet cluster formation.

We wanted to further establish that PARP-1 depletion abrogates islet cluster formation and that it was not limited to just PARP-1 KD clone 4. Hence, we used siRNA (same sequence as present in pSIP912) against PARP-1 to generate transiently PARP-1 silenced PREPs, which were then subjected to islet differentiation using both Activin A and Swertisin. Since, the islet differentiation with PREPs generated mature islets, in a mere four days it became possible to observe the effect of siRNA on islet differentiation. We observed similar results as with the stable PARP-1 clone 4 and significant abatement of islet cluster formation was observed which was confirmed by immunocytochemistry staining of NKX6.1 and c-peptide. Once we established the PARP-1 KD PREPs inability to form islet clusters we reintroduced PARP-1 by transfecting the PARP-1 KD PREPs clone 4 with a PARP-1 recovery vector which was resistant to silencing due to a point mutation where the siRNA acted. We observed a complete recovery of PREPs for their ability to form functional islet clusters which we confirmed by DTZ staining, immunostaining for c-peptide and glucagon and c-peptide release assay. This established that PARP-1 expression is vital to generate functional islets from stem/progenitors.

We repeated our study of PARP-1 KD in islet differentiation in PANC-1 cells and found similar results as previously observed in our lab (Dr. Nidheesh Dadheech thesis, 2013). We further performed a transcriptome analysis at the midpoint of the PANC-1 islet differentiation to identify possible gene targets of PARP-1 regulatory action which might overlap with results obtain from PREPs. We again found that all the key transcription factors involved in islet differentiation were significantly downregulated. Further we observed that PARP-2 expression did not change in the PARP-1 KD group suggesting it couldn't compensate for PARP-1 during islet differentiation and that the regulatory role that involves PARP-1 is highly exclusive to its own expression (de Murcia et al., 2003).

It has been previously reported that PARP-1 can interact with SMADs and modulate their action both negatively and positively (Huang et al., 2011; Lönn et al., 2010; Zhang et al., 2013). Also, TGF-β and SMAD signaling has been previously reported to be essential in signal transduction during islet

formation. Hence, in order to establish the importance of SMAD signaling in our progenitor cell model, we blocked the activation of SMAD3 by using a pSMAD3 specific inhibitor called SIS3. Since, both Activin A and Swertisin follow AKT-MEPK-TKK pathway which involve phosphorylation of pSMAD3, we observed absolute abolishment of islet cluster formation in either groups in presence of SIS3, which confirmed it being essential for islet differentiation (Dadheech et al., 2015). We also observed that undifferentiated PREPs expressed phosphorylated SMAD3 but was localised in the cytoplasm, whereas in the mature islets it translocated within the nucleus following its normal signal transduction pathway, which states that upon activation of SMAD2/3 they form a complex of pSMAD2/3 and Smad4which gets localized in the nucleus to regulate expression of target genes (Brown and Schneyer, 2010; Kim and Hebrok, 2001b). This was confirmed by fractionation study where the extra nuclear extract of the undifferentiated PREPs consisted of high expression of SMAD4 and pSMAD3 which then gets localized in the nuclear extract as the islet differentiation progressed. Similar kinetics with SMADs is observed in the embryonic endocrine pancreatic development (El-Gohary et al., 2013).

We further performed a co-immunoprecipitation during islet differentiation using PARP-1 antibody and screened for SMADs. We observed a robust interaction of pSMAD3 with PARP-1 protein which increased significantly during islet differentiation when compared to undifferentiated PREPs and PANC-1 cells. In this case PARP-1 seems to be positively modulating the action of pSMAD3 by directly interacting with it. Previous reports demonstrating PARP-1 SMAD interactions where it was reported that PARP-1 PARylates Smad3 and activates it to form Smad complex which increases the Smad3 specific gene expression (Huang et al., 2011). Conversely, in another report PARP-1 PARylated Smad3 and Smad4 which dissociated the complex from DNA abating the Smad-specific gene responses and TGF-β induced epithelial to mesenchymal transition (Lönn et al., 2010). Our results indicate that PARP-1 interacts with SMAD3, increases its phosphorylation and regulates pSMAD3 target genes essential for islet differentiation and function. Thus, could be acting as a positive regulator of pSMAD3.

Lastly, it became imperative to explore if any of the key transcription factors that downregulated due to PARP-1 knockdown are in direct transcription control of PARP-1 protein while binding to any of their promoter regions. We performed a chromatin Immunoprecipitation (ChIP) with PARP-1 antibody during islet differentiation with both Activin A and Swertisin. We observed binding of PARP-1 to the promoter sequences of Reg3a, Pdx1, Neurog3, NeuroD, Pax4 and Nkx6.1 genes suggesting that PARP-1 expression regulates the beta cell fate by controlling all the key transcription factors necessary for the differentiation and proper functioning of beta cells within islet of Langerhans. The okamoto model for Reg gene and PARP-1 regulation in pancreatic regeneration after 90% pancreatectomy in a rat model, left us with possible clue for PARP-1's transcription control in islet differentiation from stem/progenitors (Takasawa and Okamoto, 2002). The Reg promoter binding sequence of PARP-1 demonstrated by Okamoto was screened by us which was also positive for PARP-1 binding in our model system. Hence Reg promoter sequence served as an excellent positive control. This is the first report where we show transcription control activity of PARP-1 is the paradigm of islet differentiation from progenitors. It was very surprising for us to observe the binding of PARP-1 on the respective promoter regions of the six transcription factors which are key factors in the islet differentiation process. The fact that PARP-1 regulated six different genes, can be explained due to the fact that these genes have a close network where they regulate one another and have been reported to work together in a coordinated and synergistic manner in maintaining proper function of beta cells within islet of Langerhans (Andrali et al., 2008). In another report an intricate network of the above mentioned transcription factors has been shown to be tightly regulated and expressed in timely manner from early progenitors to terminally differentiated beta cells (van der Meulen and Huising, 2015). In conclusion, PARP-1 is a vital component in the transcription machinery of progenitors which regulates the key transcription factors involved in islet differentiation from PREPs to generate functional islets.

Sr. No	Gene Name (Mus musculus)	Primer Forward seq.	Primer Reverse seq.
1	**NEUROD B**	5'CGCTCAGCATCAGCAACTC3'	5'GTGGGCGAATTCCTCGTGTC3'
2	**NGN3 A**	5'AGCAGATAAAGCGTGCCAGG3'	5'CTCGCCTGGAGTAAATTGCG3'
3	**NKX6.1 A**	5'AAGAGGACGGACGATCGGAA3'	5'CGGACTAGCCGGATCGAAAA3'
4	**PAX4 A**	5'CACACATGATCTGGGGGTTGA3'	5'AGTACTGATATCGTTTCCCAGCC3'
5	**PDX1 B**	5'AGCTCATTGGGAGCGGTTT3'	5'GTGGAGCTCTCCAAAACGGG3'
6	**REG1 A**	5'CTGCAAGTTTTGCTGGGAAGT3'	5'AGACACAAGGCTCTCACCATC3'

Table 4.1: List of Primers for ChIP

Sr. No.	Antibody	Company & Catalog No.	Isotype IgG	Mono/ Polyclonal Ab	Mol. Weight (KDa)	Application	Dilution
1	Nestin	Sigma#N5413	Rabbit	Poly	177	Immunoblotting	1:1000
2	CD133	Millipore #MAB4399	Mouse	Mono	97	Immunoblotting	1:1000
3	Smad2/3	CST#8685	Rabbit	Mono	52,60	Immunoblotting	1:1000
4	Smad4	CST#9515	Rabbit	Poly	70	Immunoblotting	1:1000
5	Phospho-Smad3	CST#9520	Rabbit	Mono	52	Immunoblotting	1:1000
6	Smad7	R&D Systems #MAB2029	Mouse	Mono	50	Immunoblotting	1:500
7	p38MAPK	CST#9212	Rabbit	Poly	43	Immunoblotting	1:1000
8	Phospho-p38MAPK	CST#9216	Mouse	Mono	43	Immunoblotting	1:2000
9	Pdx-1	BD#554655	Mouse	Mono	40	Immunoblotting/Immunofluorescence	1:1000/1:200

10	Neurogenin-3	Sigma #SAB1306585	Rabbit	Poly	23	Immunoblotting/ Immunofluorescence	1:1000
11	NeuroD	CST#4373	Rabbit	Mono	49	Immunoblotting	1:1000
12	Pax-4	Sigma #AV32064-50UG	Rabbit	Mono	25	Immunoblotting	1:1000
13	MAFA	Sigma #SAB2105099	Rabbit	Mono	40	Immunoblotting	1:1000
14	Nkx 6.1	DSHB #F64A6B4	Mouse	Poly	40	Immunoblotting/ Immunofluorescence	1:40/1:20
15	GLUT2	Sigma #SAB1303865	Rabbit	Mono	61	Immunoblotting/FlowCytometry/ Immunofluorescence	1:1000/1:10/1:100
16	β-Actin	BD#612657	Mouse	Mono	42	Immunoblotting	1:10000
17	E-Cadherin	BD#610181	Mouse	Mono	120	Immunofluorescence	1:50
18	Nestin-PE	BD#561230	Mouse	Mono	177	Immunofluorescence	1:100
19	Fibronectin	Sigma#F3648	Rabbit	Poly	220	Immunofluorescence	1:400
20	Ki67	Sigma#P6834	Mouse	Mono	345 & 395	Immunofluorescence	1:400
21	CK19	Sigma#C6930	Mouse	Mono	40	Immunofluorescence	1:100
22	Insulin	CST#4590	Rabbit	Poly	6	Immunofluorescence	1:100
23	Glucagon	Sigma#G2654	Mouse	Mono	3.48	Immunofluorescence	1:100
24	CD90.2-	BD#55302	Rat	Mono		Flow Cytometry	1:10

	FITC						
25	CD44-PE	BD#553134	Rat	Mono		Flow Cytometry	1:10
26	CD34-FITC	BD#553733	Rat	Mono		Flow Cytometry	1:10
27	CD133-PE	BD#141203	Rat	Mono		Flow Cytometry	1:10
28	CD45-APC	BD#559864	Rat	Mono		Flow Cytometry	1:10
29	CD117-PE	BD#553869	Rat	Mono		Flow Cytometry	1:10
30	Vimentin	Sigma#C9080	Mouse	Mono	53	Immunofluorescence	1:400
31	Smooth muscle actin	Sigma#F3777	Mouse	Mono	42	Immunofluorescence	1:250
32	C-Peptide	CST#4593	Rabbit	Mono	5	Immunofluorescence	1:100
33	PARP-1	Santacruz# SC-1561	Goat	Poly	116	IP and ChIP and Immunoflorescence	1ug/1:50
34	PARP	CST#9532	Rabbit	Mono	116,89	WB	1:1000
35	PARP-2	Millipore# MABE18	Mouse	Mono	62	WB	1:1000
36	Erk1/2	CST#9102	Rabbit	Poly	42/44	WB	1:1000
37	Anti-Mouse-IgG-	Jackson ImmunoResearch #115-035-003	Goat	Poly		Immunoblotting	1:5000
38	Anti-Rabbit-IgG-HRP	Jackson Immuno Research	Goat	Poly		Immunoblotting	1:5000

		#111-035-003					
39	Anti-Mouse-IgG-FITC	Sigma#F8771	Goat	Poly		Immunofluorescence	1:200
40	Anti-Rabbit-IgG-FITC	Sigma#F9887	Goat	Poly		Immunofluorescence	1:200
41	Anti-Mouse-IgG-CF555	Sigma#SAB4600299	Goat	Poly		Immunofluorescence	1:100
42	Anti-Rabbit-IgG-CF555	Sigma#SAB4600068	Goat	Poly		Immunofluorescence	1:100
43	Goat IgG	Jackson#111-035-003	Rabbit	Poly		IP and ChIP	1ug

Table 4.2: List of Antibodies.